Accepted Manuscript

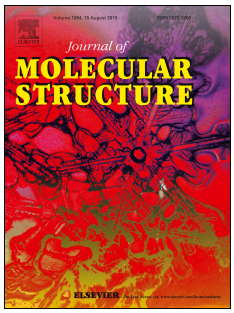

Spectroscopic, thermal, catalytic and biological studies of Cu(II) azo dye complexes

A.Z. El-Sonbati, M.A. Diab, A.A. El-Bindary, A.F. Shoair, M.A. Hussein, R.A. El-Boz

PII: S0022-2860(17)30370-8

DOI: 10.1016/j.molstruc.2017.03.082

Reference: MOLSTR 23578

To appear in: *Journal of Molecular Structure*

Received Date: 17 December 2016

Revised Date: 20 March 2017

Accepted Date: 21 March 2017

Please cite this article as: A.Z. El-Sonbati, M.A. Diab, A.A. El-Bindary, A.F. Shoair, M.A. Hussein, R.A. El-Boz, Spectroscopic, thermal, catalytic and biological studies of Cu(II) azo dye complexes, *Journal of Molecular Structure* (2017), doi: 10.1016/j.molstruc.2017.03.082.

Spectroscopic, thermal, catalytic and biological studies of Cu(II) azo dye complexes

A.Z. El-Sonbati [1,+], M.A Diab[1], A.A. El-Bindary[1], A.F. Shoair [1], M.A. Hussein[2] and R.A. El-Boz[1]

[1]Department of Chemistry, Faculty of Science, Damietta University, Damietta, Egypt
[2]Department of Chemistry, Faculty of Science, Port Said University, Port Said, Egypt

Abstract

New complexes of copper(II) with azo compounds of 5-amino-2-(aryl diazenyl)phenol (HL_n) are prepared and investigated by elemental analyses, molar conductance, IR, ^{1}H-NMR, UV-Visible, mass, ESR spectra, magnetic susceptibility measurements and thermal analyses. The complexes have an square planar structure and general formula $[Cu(L_n)(OAc)].H_2O$. Study the catalytic activities of Cu(II) complexes toward oxidation of benzyl alcohol derivatives to carbonyl compounds were tested using H_2O_2 as the oxidant. The intrinsic binding constants (K_b) of the ligands (HL_n) and Cu(II) complexes (**1-4**) with CT-DNA are determined. The formed compounds have been tested for biological activity of antioxidants, antibacterial against Gram-positive (*Staphylococcus aureus*) and Gram-negative (*Escherichia coli*) bacteria and yeast *Candida albicans*. Antibiotic (Ampicillin) and antifungal against (Colitrimazole) and cytotoxic compounds HL_1, HL_2, HL_3 and complex (1) showed moderate to good activity against *S. aureus*, *E. coli* and *Candida albicans*, and also to be moderate on antioxidants and toxic substances. Molecular docking is used to predict the binding between the ligands with the receptor of breast cancer (2a91).

Keywords: Azo compound, Cu(II) complexes; DNA binding; Biological activity; Thermal analysis.

+ Corresponding author: E-mail address: elsonbatisch@yahoo.com (A.Z. El-Sonbati).

1. Introduction

It has already been a number of organic dyes unified innovations of our day-to-day life. Azo dyes are hardly organic compounds biodegradable because of its high stability to light and resistant to microbial attack. The greater part of the azo compounds are a class of synthetic aggravates that are continuously getting consideration in experimental exploration [1,2]. Azo dyes can supply a complete rainbow of colors; therefore they have tremendous importance as dyes and also as

pigments for a long time [3]. Azo dyes are generally synthesized by the reaction of primary aromatic amines by diazotization and coupling with phenol or secondary aromatic amines. In fact, about half of the dyes in the industry are also compounds, which are mostly prepared from diazonium salts [4-6]. Azo compounds as organic dyes have attracted considerable attention due to their applications [7,8].

Azo dye compounds coordinate with metal ions depend on the nature of the metal, their valence, the number of donor atoms within the ligand, the type of chelating rings formation and pH of the reaction medium. It is known that azo dye compounds and their metals complexes are known to be involved in a number of biological reactions, such as the inhibition of DNA, RNA, synthesized protein, nitrogen fixation and carcinogenesis [9-11].

Herein, we describe the synthesis and characterization of 5-amino-2-(aryldiazenyl) phenol (HL_n) and their Cu(II) complexes by different spectroscopic techniques. Calf thymus DNA-binding activity of the ligands and copper(II) complexes were studied by absorption spectra. Catalytic oxidation of benzyl alcohol derivatives to the corresponding carbonyl compounds in presence of the formed complexes using H_2O_2 as oxidant was studied. The optimal bond lengths and bond angles has been investigated and calculated.

2. Experimental

2.1. Materials

3-Aminophenol obtained from Aldrich Chemical Company was used without any further purification. Aniline (99.5%), 4-derivatives anilines (alkyl: CH_3 (96.0%), Cl (98.0%) and NO_2 (97.0%); and copper acetate ($CuOAc.H_2O$) from Sigma. All other used chemicals and solvents were of analytical reagent grade.

2.2. Synthesis of the ligands and their complexes

2.2.1. Synthesis of the azo dye ligands (HL_n)

The ligands of 5-amino-2-(aryldiazenyl) phenol (HL_n) were prepared by dissolving aniline or its *p*-substituted derivatives (10 mmol) in conc. H_2SO_4 diazotized compound below -5 ° C in an ice - salt bath with sodium nitrate solution (0.8 g 0.10 mmol and 30 mL distilled H_2O). Diazonium salt was coupled with an alkaline solution of 3- aminophenol (1.0 g 0.10 mmol) in 20 ml of ethanol. The precipitate was filtered and dried after through rinsing with water and ethanol mixture. The crude product was recrystallized from ethanol and the microcrystals were obtained in a yield of 94-98 %. The resulting formed ligands (Fig. 1) are:

HL_1= 5-amino-2-(*p*-methyl phenyl diazenyl) phenol.

HL_2 = 5-amino-2-(phenyldiazenyl) phenol.

HL_3 = 5-amino-2-(*p*-chlorophenyl diazenyl) phenol.

HL_4= 5-amino-2-(*p*-nitro phenyl diazenyl) phenol.

2.2.2. Synthesis of Cu(II) complexes (1-4)

Copper(II) complexes were prepared (Fig. 2) according to the general procedures described by El-Sonbati et al. [8,12]. A stoichiometric amount of the desired ligand (0.02 mol) in ethanol (20 mL) was added dropwise to a hot ethanol solution (20 mL) of $CuOAc.H_2O$ (0.01 mol) and the reaction mixture was refluxed for 6 hours. The solution was concentrated and the microcrystalline solid separated, which was isolated by filtration, washed with hot ethanol, ether and dried in a vacuum dryer over anhydrous $CaCl_2$.

2.2.3. DNA binding experiments

Binding characteristics of ligands and CT-DNA complexes have been studied using electronic absorption spectroscopy. The stock solution of CT-DNA was prepared in 5 mM Tris-HCl/50 mM NaCl buffer (pH=7.2), which a ratio of UV absorbance's at 260 and 280 nm (A_{260}/A_{280}) of ca. 1.8-1.9, showing that the DNA was adequately free of protein [13, 14]. Furthermore, the fixation was dictated by UV absorbance at 260 nm ($\mathcal{E}$= 6600 M^{-1} cm^{-1}) [15]. Electronic absorption spectra (200-700 nm) were carried out using 1 cm quartz cuvettes at 25 ^{o}C by fixing the concentration of ligand or complex (1.00×10^{-3} mol L^{-1}), with a gradual increase in the concentration of CT-DNA (1.30×10^{-4} mol L^{-1}). The intrinsic binding constant K_b of the compound with CT-DNA was determined using the following equation [8,16]:

$$[DNA] / (\epsilon_a-\epsilon_f) = [DNA] / (\epsilon_b-\epsilon_f) + 1 / K_b(\epsilon_a-\epsilon_f)$$

Where [DNA] is the concentration of CT-DNA in base pairs, ϵ_a is the extinction coefficient observed for the A_{obs}/[compound] at the given DNA concentration, ϵ_f is the extinction coefficient of the free compound in solution and ϵ_b is the extinction coefficient of the compound when fully bond to DNA. In plots of $[DNA]/(\epsilon_a-\epsilon_f)$ versus [DNA], K_b is given by the ratio of the slope to the intercept.

2.2.4. Catalytic oxidation of alcohols by Cu(II) complex

The complex $[Cu(L_1)(OAc)]$ H_2O (0.0064 g, 0.01 mmol) was dissolved in DMF (2 mL) and H_2O (10 mL), then benzyl alcohol (2 mmol) was added with stirring for 30 min. Hydrogen peroxide (2.3 mL, 30%, 10 mmol) was then added dropwise and reaction mixture was irradiated ultrasonically for further 30 min then reduced in vacuum. The carbonyl compound extracted by diethyl ether (3×10 mL), filtered through a bead of silica gel and dried over anhydrous $MgSO_4$. The produced benzaldehyde were quantified as 2,4-dinitrophenylhydrazone derivative.

2.2.5. Biological Studies

2.2.5.1 Antioxidant activity screening assay ABTS method

For each of the investigated ligands (HL_n) and their complexes, 2 mL of 2,2'- azino-bis (3-ethylbenzthiazoline-6-sulphonic acid (ABTS) solution (60 µM) was added to 3 mL MnO_2 solution (25 mg/mL) in 5 mL aqueous phosphate buffer solution (pH 7, 0.1 M). The mixture was shaken, centrifuged, filtered, and the average absorbance of the resulting green blue solution at 734 nm was adjusted to about ca. 0.5. Then, 50 µl of 2 mM solution of test compound in spectral grade MeOH / phosphate buffer (1: 1) was added. The absorbance measurement at 734 nm decrease in color intensity was expressed as percentage of inhibition [17].

2.2.5.2. Antibacterial activity

Chemical compounds were individually tested against a gram positive (*Staphylococcus aureus*), gram negative (*Escherichia coli*) bacteria and yeast (*Candida albicans).* 1 mg of each compound was dissolved in 1 mL DMSO and the solution was placed in petri dish containing a sterilized Whatman filter paper (5 cm) and media nutrient agar (beef extract 3 g meat + peptone 5 g and 20 g agar) seeded with the tested microorganisms. The petri dishes were incubated at 35˚C and the inhibition zones were recorded after 24 h. Each treatment was replicated three times. The antibacterial activity of standard antibiotic (ampicillin) and antifungal (colitrimazole) was also recorded using the same procedure as above at the same concentration and solvents. The % activity index for the complex was calculated by the formula as follows:

$$\% \text{ Activity index} = \frac{\text{Zone of inhibition by test compound (diameter)}}{\text{Zone of inhibition by standard (diametre)}} \times 100$$

2.2.5.3. Antitumor activity

The cell lines hepatocellular carcinoma (HePG-2) and mammary gland breast cancer (MCF-7) were used to determine the inhibitory effects of compounds on cell growth using 3-[4,5-dimethylthiazol-2-yl]-2,5-diphenyl tetrazolium bromide (MTT) assay. Solutions of MTT, dissolved in medium or balanced salt solutions without phenol red, are yellowish in color. Mitochondrial dehydrogenases of viable cells cleave the tetrazolium ring, yielding purple formazan crystals which are insoluble in aqueous solutions. Cell lines were cultured in with 10% fetal bovine serum. Antibiotics added were 100 units/ml penicillin and 100 µg/mL streptomycin at 37 ^{o}C in a 5% CO_2 incubator. The cell lines were seeded in a 96-well plate at a density of 1.0×10^4 cells/well for 48 h under 5% CO_2. After incubation, the cells were treated with different concentration of compounds and incubated again for 24 h. After 24 h of drug treatment, 20 µL of MTT solution were added from concentrations range 1.56-100 µg/mL and incubated for 4 h. Dimethyl sulfoxide (DMSO) in volume of 100 µl is added

into each well to dissolve the purple formazan formed. The colorimetric assay is measured and recorded at absorbance of 570 nm using a plate reader (EXL 800). The relative cell viability percentage was calculated as (A570 of treated samples/A570 of untreated sample) × 100 [18].

2.2.6. Molecular docking

Docking calculations were carried out using Docking Server. The MMFF94 force field was used for energy minimization of ligands molecule using Docking Server. Gasteiger partial charges were added to the ligand atoms. Non-polar hydrogen atoms were merged, and rotatable bonds were defined.

Docking calculations were carried out on 2a91 – SIGNALING PROTEIN, TRANSFERASE, MEMBRANE PR protein model. Essential hydrogen atoms, Kollman united atom type charges, and solvation parameters were added with the aid of AutoDock tools. Affinity (grid) maps of 20×20×20 Å grid points and 0.375 Å spacing were generated using the Autogrid program. AutoDock

Parameter set- and distance-dependent dielectric functions were used in the calculation of the van der Waals and the electrostatic terms, respectively.

Docking simulations were performed using the Lamarckian genetic algorithm (LGA) and the Solis & Wets local search method. Initial position, orientation, and torsions of the ligand molecules were set randomly. Each docking experiment was derived from 10 different runs that were set to terminate after a maximum of 250000 energy evaluations. The population size was set to 150. During the search, a translational step of 0.2 Å, and quaternion and torsion steps of 5 were applied [19-22].

2.2.7. Analytical techniques

2.2.7.1. Infrared spectroscopy (IR)

IR spectra (KBr discs, 4000-400 cm^{-1}) by recorded in Jasco FTIR-4100 spectrophotometer.

2.2.7.2. ^{1}H- Nuclear magnetic resonance spectroscopy (^{1}H- NMR)

The ^{1}H- NMR spectra were recorded by Bruker WP 300 MHz using DMSO-d_6 as a solvent containing TMS as the internal standard.

2.2.7.3. UV–Visible spectroscopy

UV–Visible spectra were recorded by Perkin-Elmer AA800 spectrophotometer Model AAS.

2.2.7.4. Magnetic susceptibility measurements

Magnetic susceptibility measurements has been identified at room temperature on the balance of the magnetic susceptibility Johnson Matthey using mercury $Hg[Co(SCN)_4]$ as calibration.

2.2.7.5. Thermogravimetric analysis (TGA)

TGA of the ligands and copper complexes were carried out using Shimadzu thermogravimetric analyzer under nitrogen atmosphere with a heating rate of 15 ^{o}C / min at a temperature ranging from room temperature up to 800 °C.

2.2.7.6. Microanalysis

Elemental microanalyses of the compounds for C, H, and N were determined on Automatic Analyzer CHNS Vario ELIII, Germany. The analyses were repeated twice to check the accuracy of the analyzed data. The metal content in the complexes was estimated by standard methods [12].

2.2.7.7. X-ray diffraction analysis

X-ray diffraction analyses of the powder form of Cu complexes were performed [23] at room temperature by a Philips X-ray diffractometer equipped with utilized monochromatic Cu K_α radiation (λ = 1.540598 Å). The X-ray tube voltage and current were 40 kV and 30 mA, respectively.

2.2.7.8. Molecular structure investigations

The molecular structures of the investigated compounds were optimized by HF method with 3-21G basis set. The molecules were built with the Perkin Elmer ChemBio Draw and optimized using Perkin Elmer ChemBio 3D software [24].

2.2.7.9. ESR measurements

ESR measurements of powdered samples were recorded at room temperature using an X-band spectrometer utilizing a 100 kHz magnetic field modulation with diphenyl picrylhydrazyle (DPPH) as a reference material. The conductance measurement was achieved using Sargent Welch scientific Co., Skokie, IL, USA.

3. Results and discussion

The ^{1}H NMR spectrum of HL_2 was recorded in DMSO-d_6 solution using TMS as internal standard **(Fig. S1)**. The compound under investigation show a signal at δ 10.00 ppm, which can be assigned to the phenolic –OH group proton with integration equivalent to one proton. The compound shows a group of multiple-signals corresponding to the aromatic protons δ5.95-6.35 and δ7.35-7.80 ppm. Also, the spectrum show a single at δ 6.62 ppm (s; 2H, NH_2) due to the two protons of amino group in *p*-position to the N=N group. The ligand show a signal at δ12.45 ppm, which may be attributed to the presence of intramolecular

hydrogen bond between the phenolic –OH group of the moiety in HL_2 and the azodye group. on addition of D_2O the intensities of both OH and NH_2 protons significantly decrease **(Fig. S1(b))**. The peak at (10.30/12.45) ppm, which is due to the exchangeable hydrogen-bonded hydroxyl (OH) proton, disappears upon exchange with D_2O and can be associated with the–OH proton involved in intramolecular hydrogen bonding with the azodye nitrogen atom [25].

Analytical data indicates that the diazo coupling reaction between 3- aminophenol and aniline or its *p*-substituted derivatives occurs in 1 : 1 molar ratio and the product form well defined complexes with $Cu(OAc)_2.2H_2O$. Formation of the complexes can be represented by the following equation.

$$Cu(OAc)_2.2H_2O \quad + \quad HL_{1\text{-}4} \quad \rightarrow \quad [Cu(L_{1\text{-}4})(OAc)]H_2O + CH_3COOH$$

Formulation of the complexes (1-4) has been based on their elemental analytical data, molar conductance, magnetic susceptibility data and different spectroscopic techniques. The results are consistent with 1 : 1 metal:ligand stoichiometry (**Table 1**). The azo dye ligands and their complexes are soluble in all common organic solvents, non-hygroscopic. The conductance measurements, recorded for 10^{-3} M solutions of the complexes in DMSO show that copper(II) complexes are non-electrolytes. Hence the one acetate in copper(II) complexes are in the coordination sphere and confirmed by analytical data.

The values of the yield (%) and the melting point are related to the nature of the *para* substituent as they increased according to the following order: *p*-(NO_2 > Cl > H > CH_3). This can be attributed to the fact that the charge effectively increased due to the electron withdrawing substituent (HL_4), while it decreased by electrons donating character of HL_1, HL_3 and HL_2 ligands. This is in accordance with that expected from Hammett's constant (σ^R) as shown in (**Fig. S2(a,b)**) correlate the yield (%) and melting point values with σ^R, it is clear that all these values increase with increasing σ^R.

3.1. IR spectra

The IR spectra of the complexes are compared with those of the free ligands (HL_n) in order to determine the coordination sites that may be involved in chelation. These peaks, such as those of OH, N=N, and NH_2, are expected to be involved in chelation. The position and/or the intensities of the peaks are expected to be changed upon chelation. On examining these spectra by comparison with the free ligands, one can conclude the following, all complexes under investigation exhibit a υ_a(COO) is observed at 1585 cm^{-1} and υ_s(COO) at 1400 cm^{-1} apart from the skeletal vibrations of the ligands. The separation between these two frequencies ($\Delta\upsilon$ = 185 cm^{-1}) adequately supports bidentate coordination of the acetato

group [8]. The broad band υ(O-H) water is absent in the spectrum of the ligand (HL_n), but is present in the complexes at 3185-3360 cm^{-1} [8,26] **(Fig. S3)**.

The IR spectra of the ligands (HL_n) exhibit a broad medium intensity band ranging from 3100-3500 cm^{-1} with peak centered at ~3370±12 cm^{-1} which can be assigned to the stretching vibration of phenolic (O-H) group [8]. The disappearance of the υ(O-H) phenolic and a medium intensity bands at 1260-1220 cm^{-1} can be attributed to υ(C-O) vibration of C-O-H group [7,27], supports the contribution that proton displacement from the phenolic –OH groups through the metal ion forming a bond link between the oxygen of the phenolic group and the metal ion. A band appearing at 1466 cm^{-1} assigned to υ(N=N) is shifted to lower frequency on complex formation by 8-17 cm^{-1}, showing that the coordination through one of the azo nitrogen atom [8]. New bands in all complexes at 580-624 and 407-470 cm^{-1} are assigned to υ(Cu-O) and υ(Cu-N), respectively. The υ(NH_2) in all ligands under investigation still lie at the same position in the spectra of the complexes.

3.2. Mass spectra

The electron impact mass spectra of ligand (HL_3) and its complex (3) are recorded and investigated at 70 eV of electron energy. It is obvious that, the molecular ion peaks are in good agreement with their suggested empirical formula as indicated from elemental analyses (**Table 1**). The mass spectra fragmentation mode of the ligand HL_3 shows the exact mass of ligand is 247.5 corresponding to the formula $C_{12}H_{10}N_3OCl$ and mass of its complex 387.28 corresponding to the formula $CuC_{14}H_{14}N_3O_4Cl$ as shown in **Fig. S4(a and b)**, respectively. The ion of ligand m/z = 247.5 undergoes fragmentation to a stable peak at m/z = 219.5 by losing N_2 atoms (structure **I**) as shown in **Fig. 3**. The loss of Cl leads to the fragmentation with m/z = 184 (structure **II**). The loss of NH_2 atoms leads to the fragmentation with m/z = 168 (structure **III**). A breakdown of the backbone of HL_3 ligand gives the fragment **(IV).** The mass spectrum fragmentation modes of complex (3) shows the m/z=387.046 and undergoes fragmentation to stable at m/z =214.5 by losing H_2O, Cu, OAc and ONH_2 (structure **I)** as shown in **Fig. 4**. The loss of N_2 leads to fragmentation with m/z = 186.5 (structure **II**). A breakdown of the backbone of complex gives the fragments **(III).**

3.3. X-ray diffraction

The X-ray diffraction (XRD) patterns for the powder form of complexes $[Cu(L_1)(OAc)]H_2O$ (1) and $[Cu(L_4)(OAc)]H_2O$ (4) are presented in **Fig. 5**. The XRD show many diffraction peaks which confirm the polycrystalline phase while the complex $[Cu(L_2)(OAc)]$ H_2O (2) is amorphous/polycrystalline mixture phase. The average crystallite size (ξ) and The dislocation density (δ) can be calculated from the XRD pattern according to following equation [23]:

$$\xi = \frac{K\lambda}{\beta_{1/2}\cos\theta},$$

$$\delta = \frac{1}{\xi^2}$$

where λ is wavelength of X-ray radiation (1.540598 Å), K is a constant taken as 0.95 for organic compounds and $\beta_{1/2}$ is full width at half maximum of the reference diffraction peak measured in radians and θ is the angle of diffraction. The calculated values of ξ are found 241 and 270 nm for complex (1) and complex (4), respectively. The calculated values of δ are found to be 1.72×10^{-3}, 1.37×10^{-5} nm^{-2} for complexes (1) and (4), respectively**.** The diffraction peaks in powder spectra are indexed and the lattice parameters are determined with the aid of CRYSFIRE computer program [28]. The optimum indexed Miller indices, (*hkl*), for complexes under investigation are determined by using CHEKCELL program [29] and presented in **Fig. 5**. The calculated lattice parameters which are a, b, c, α, β and γ in addition to crystal system and space group are presented in **Table 2**.

3.4. Thermal analyses

Thermal analysis by the TGA techniques has proved to be very useful in determining the crystal water content in complexes and the percentage of loss of masses of the ligands and their thermal stability. The experimental results showed that the thermal decomposition of ligands (HL_n) and their Cu (II) complexes included two and three main steps, respectively. The determined temperature ranges and the corresponding percent mass losses are given in **Table S1 (Figs. S5 and S6).**

HL_1 ligand shows two decomposition steps, the first stage occur in the temperature range 30-342 ^oC is attributed to loss of a part of the ligand ($C_7H_7N_2$) (Found 50.31 % and Calc. 52.42%). The second stage in the temperature range 342-806 ^oC loss of a part of the ligand C_6H_6NO (Found 49.69% and Calc. 47.57%). The determined temperature ranges and the corresponding percent mass losses are given in **Table S1**.

All Cu (II) complexes (1-4) showed TG curves in the temperature range ~30-400 °C loss of outer H_2O molecule followed by loss of CH_3COO molecule. The third stage is related to loss of the part of ligand. The final weight losses are due to the decomposition of the rest of the ligand and metal oxides residue (**Table 3**).

3.5. Thermodynamic parameters for thermal degradations

The thermodynamic activation parameters of decomposition processes of the ligands (HL_1, HL_2, HL_3 and HL_4) and their Cu (II) complexes (**1**, **2, 3** and **4**) namely activation energy (E_a), enthalpy (ΔH^*), entropy (ΔS^*), and Gibbs free energy change of the

decomposition (ΔG^*) are evaluated graphically by employing the Coast-Redfern [30] and Horowitz-Metzger [31] methods and drown of Coats–Redfern (CR) and Horowitz-Metzger (HM) of the ligands (HL_n) and their Cu(II) complexes (1-4) (**Figs. 6 and 7**), respectively. The calculated values of E_a, A, ΔS^*, ΔH^* and ΔG^* for the decomposition steps for ligands and complexes are summarized in **Table 4**. According to the kinetic data obtained from TGA curves, the negative values of activation entropies ΔS^* indicate more ordered activated complexes than the reactants. It was found that the thermal stability of the metal complexes was higher than that of the ligands.

3.6. Molecular structure

Molecular structures for ligands (HL_n) and their complexes are shown in **Fig. 8**. Molecular structures (HOMO & LUMO) are presented in **Fig. S7**. Selected geometric parameter bond lengths and bond angles are tabulated in **Tables S2-S5 and 5-8** for the ligands HL_n and their complexes, respectively. The HOMO–LUMO energy gap (ΔE) is an important stability index which is applied to develop theoretical models for explaining the structure and conformation barriers in many molecular systems. The calculated quantum chemical parameters are given in **Table 9**, global electrophilicity, ω, global softness, *S* and additional electronic charge, and ΔN_{max}, have been calculated [8]. It seems that the electronegativity (χ) of complexes higher than ligands and electronegativity (χ) of ligands increase from HL_1 to HL_4 and also electronegativity of complexes increased. This can be attributed to the fact that the effective charge increased due to the electron withdrawing *p*-substituent (HL_3 and HL_4) while it decreased by the electrons donating character of (HL_1).

3.7. Molecular docking

Breast cancer rates gradually increased since the 1940s in many industrialized countries. HER2 is a member of the epidermal growth factor receptor (EGFR / ERBB) family. Amplification of this oncogene has been shown to play an important role in the development and progression of some aggressive types of breast cancer. In recent years, the protein biomarker becomes important goal of treatment for about 30% of breast cancer patients [32].

Results of docked ligands were analyzed with the 2a91 as shown in **Fig. S8 (A and C).** The results showed a possible arrangement between ligands (HL_n) and receptor (2a91). The docking study showed a favorable interaction between ligands HL_n and the receptor 2a91 and the calculated energy is listed in **Table S6** and **Fig. S8 (A and C)** for receptor 2a91, respectively. According to the results obtained in this study, HB plot curve indicate that, the ligands HL_n binds to the protein with hydrogen bond interactions and decomposed interaction energies in Kcal/mole were exist between the of ligands HL_n with (2a91) receptor as shown in **Fig. 9** and **Table S7**. The ligands (HL_n) have a great affinity (pk_I) for

(2a91) receptor as shown in **Table S6**. The calculated efficiency is favorable where Ki values estimated by AutoDock were compared with experimental K_I values, when available, and the Gibbs free energy is negative. Also, based on this data, we can propose that interaction between the (2a91) receptor and the ligands (HL_n) is possible. 2D plot curves of docking with ligands (HL_n) are shown in **Fig. S9**. Binding energies are most widely used as mode of measuring binding affinity of a ligands. Thus, decrease in binding energy due to mutation will increase the binding affinity of the azodye ligands toward the receptor. As the electron density on azo dye group decrease the bending of our ligands with the receptor (2a91) increase, ($HL_4 > HL_3 > HL_2 > HL_1$). The characteristic feature of azo dye ligands was represented in presence of several active sites available for hydrogen bonding. This feature gives them the ability to be good binding inhibitors to the protein and will help to produce augmented inhibitory compounds. The results confirmed also that, the azo dye ligands derived from 3-aminophenol is efficient inhibitor of 2a91.

3.8. Magnetic measurement and electronic spectra

The room temperature magnetic moment values (μ_{eff}) per copper ion for the complexes were 0.93-1.99 BM range which may suggest a square planar structure [33]. The observed magnetic moments of the complexes are consistent with the presence of single unpaired electron [34,35]. The electronic absorption spectra of the ligands and its copper complexes were measured at room temperature in DMF solutions. The electronic absorption spectra of the ligands display one electronic absorption in the ranges 22222-21460 cm^{-1}, which are assigned to $n \rightarrow \pi^*$ and intraligand $\pi \rightarrow \pi^*$ transitions, respectively. The electronic spectra of the copper (II) complexes display two electronic absorption bands in the ranges 17915-17430 and 19300-20410 cm^{-1}, assignable to the transition $^2B_{1g} \rightarrow {}^2A_{1g}$ and $^2B_{1g} \rightarrow {}^2E_g$ indicating the possibility of a square planar complexes. These spectral features support the square planar geometry around copper (II) center [33]. Additional bands are present in the high-energy region are assignable to (O → Cu) and (N=N → Cu) charge-transfer transitions [36]. These spectral features are in agreement with the other square planar copper(II) complexes [37].

3.9. ESR spectra

To obtain further information about the stereochemistry and the site of the metal ligand bonding and to determine the magnetic interaction in the metal complexes. ESR spectral assignments of the Cu (II) complexes along with the spin Hamiltonian and orbital reduction parameters are summarized in **Table 10**. The ESR spectra of the complexes (1-3) have been studied to provide information about the hyperfine and super hyperfine structures to elucidate the geometry and the degree of covalence of the metal-ligand bond. The spectra of the complexes (1-3) show typical axial behavior with slightly different g_{ll} and g_l values.

The various Hamiltonian parameters have been calculated for these complexes (1-3) (**Table 10**). The ESR spectra of copper(II) complexes exhibits axially symmetric g-tensor parameters with $g_{ll} > g_{\perp} > 2.0023$ indicating that the copper site has a d_{x2-y2} ground state, characteristic of square planar geometry and axially symmetric [38]. It has been reported that g_{ll} value of copper(II) complexes can be used as a measure of the covalent character of the metal-ligand bond. If the value is more than 2.3, the metal-ligand bond is essentially ionic and the value less than 2.3 is indicative of covalent character [39]. The present ESR results show that g_{ll} is lower than 2.3 in this case suggesting that the copper (II) complexes are covalent in nature [40]. Also the trend $g_{ll} > g_{\perp} > g_{av}$ observed for these complexes indicate that the unpaired electron is most likely in the d_{x2-y2} orbital of the copper(II) ion and are characteristic for the axial symmetry [41]. In axial symmetry, the g-values are related to the G-factor by the expression $G = (g_{ll}-2)/(g_{\perp}-2) = 4$. According to Hathaway and Billing [41], if the value of G is greater than 4, the exchange interaction between copper (II) centers in the solid is negligible, whereas when it is less than 4, a considerable exchange interaction exists in the solid complex. The calculated G values (**Table 10**) lie within the range 3.90 – 5.44 for the copper (II) complexes (1-3). This support the absence of exchange coupling between copper (II) centers in the solid state [42]. The f is taken as in indication for the stereochemistry of the copper (II) complexes. Addition has suggested this ratio may be an empirical indication of the tetrahedral distortion of the square planar geometry. The values lower than 135 cm^{-1} are observed for square planar structures and those higher than 150 cm^{-1} for tetrahedral distortion complexes. The values for the complexes under investigation, **Table 10**, showed that all complexes associated with a square planar ligand field around the copper(II) centers.

Molecular orbital coefficient, α^2 (a measure of the covalence of the in-plan σ-bonding between a copper 3d orbital and the orbitals) and β^2 (covalent in-plan π-bonding) was calculated [43-48], which may be regarded as measure of covalence of the in-plane σ-bonding, in-plane π-bonding and our of plane π-bonding, respectively. The value of $\alpha^2 = 1.0$ indicates complete ionic character, whereas $\alpha^2 = 0.5$ denotes 100% covalent bonding, with the assumption of negligible small values of the overlap integral. According to Hathaway [49,50], the calculated values of K^2_{ll}, $K^2_{\perp}$ and K^2, **Table 11**, showed that $K_{ll} \approx K_{\perp} \approx 0.77$ for pure in-plane σ-bonding and $K_{ll} < K_{\perp}$ for in-plane π-bonding, while for out of plane π-bonding $K_{ll} > K_{\perp}$. In all the Cu(II) complexes, it is observed that $K_{ll} < K_{\perp}$ which indicates the presence of significant in-plane π-bonding. The values of bonding parameters α^2 and $\beta^2 < 1.0$ indicate significant in-plane σ-bonding and in plane π-bonding. It was found that the values of β^2, α^2, g_{ll} and G of Cu(II) complexes **(1-3)** g_{ll}, $A_{ll} \times 10^{-4}$ cm^{-1} and β^2 values are

dependent of the substituents effect of the *p*-position of the ligand and can be order as: *p*-(Cl > H > CH_3) as shown in **Fig. 10**.

3.10. Catalytic oxidation of alcohols

Copper (II) complexes have been well investigated in catalyzing the selective oxidation of alcohols to aldehydes in the past decade [51,52]. Compared to the other transition metal compounds, copper catalysts are commercially inexpensive, easily to be prepared and handled. Although some Cu(I)/Cu(II) salts and their composites [53] have shown good catalytic activity towards such reactions, the coordination compounds of copper with various ligands are mostly investigated because of the solubility, the steric hindrance, the stability and the redox properties of these catalysts could be easily adjusted by the ligands used [54-56].

However, catalytic methods based on transition metals need stringent reaction conditions and high cost of the ligand, or have the disadvantages like long reaction time and high temperature. Therefore, the development of practical, inexpensive, simple and green chemical process for oxidation is still needed. We are interested in the use of hydrogen peroxide, since it is cheap and sufficiently environment-friendly to be used on a commercial scale. Herein, we investigate the catalytic oxidation of benzyl alcohol by the catalyst system, $[Cu(L_1)(OAc)]H_2O/H_2O_2$ at room temperature. As a typical reaction procedure, oxidation experiments have been performed as follows: 10 mmol of 30% H_2O_2 was added drop wise to the solution of the complex (0.01 mmol) and alcohol (2 mmol) in a mixture of DMF and H_2O as solvents and the reaction mixture irradiated ultrasonically for 0.5 h. The color of the reaction mixture changes from brown to green; this is probably due to coordination of the alcohol to the copper (II) ion.

However, oxidation of benzyl alcohol in 80% with turnover frequency (TOF) 10.6 h^{-1}. The catalytic oxidation of benzyl alcohol as a model substrate has been performed in the absence of $[Cu(L_1)(OAc)]$ H_2O and in the presence of some other co-oxidants like $NaIO_4$, $K_2S_2O_8$, $NaBrO_3$ and NaOCl instead of H_2O_2 and gave very low yield of benzaldehyde (less than 5%). This is probably due to the formation of the solid precipitates $NaIO_3$, K_2SO_4, NaBr and NaCl, respectively, which remain at the end of the reaction and make the workup, is difficult. We conclude that the use of $[Cu(L_1)(OAc)]H_2O$ is preferred catalyst for oxidation of benzyl alcohol to benzaldehyde. The mechanism of this reaction could be explained on the basis of the catalytic cycle shown below. Hydrogen peroxide oxidizes the produced Cu(I) ion to Cu(II) ion again which in turn oxidizes the remaining benzyl alcohol. This catalytic cycle continue till all the substrate is completely consumed. The novelty in this technique towards this complex has not been tested before for this catalytic oxidation reaction in addition, this catalytic system is good for catalytic oxidation of these compound since (1) it works at room temperature, (2) the yield is comparable to other catalytic systems, (3) the work-up is simple and (4) reaction time is short.

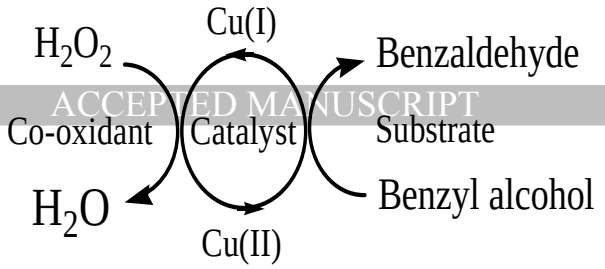

3.11. Biological studies

3.11.1. ABTS antioxidant activity

The antioxidant activities of azo ligands and its metal complexes were evaluated by in vitro methods in order to compare the results. The evaluation study was carried out with different concentrations of ligand and metal complexes and ascorbic acid was used as a standard.

By comparing the results obtained of antioxidant of the azo ligand compounds reported in this study compounds HL_1, HL_2 , HL_3 and complex (1) showed high antioxidant activity in the sequence $HL_1 > HL_2 > HL_3 > HL_4$ according to decreasing of electronegativity on azo group (**Table 11**). Also we found that copper complex of ligand HL_1 is the only complex which increase the antioxidant activity than its ligand.

3.11.2. Antibacterial activity

The diseases caused by microbial infections were a serious menace to the health of human being and often have connection to some other diseases when the body system gets debilitated. Developing antimicrobial drugs and maintaining their potency in opposition to resistance by different types of microorganisms as well as a broad spectrum of antibacterial and antifungal activities were of major concerns of research in this area.

Antimicrobial activity of the synthesized compounds were screened in *vitro* against gram positive and gram negative bacterial and a yeast in comparison with control drugs ampicillin as an antibacterial agent and colitrimazole as an antifungal agent, by the agar diffusion technique [57,58]. Biological evaluation *in vitro* revealed that compounds HL_1, HL_2, HL_3 and complex (1) exhibited moderate to slight inhibitory action activity against *Staphylococcus aureus* and Escherichia *coli*. The rest of compounds showed slight to no sensitivity at all to the tested microorganisms. Complex (1) showed good activity against *E. coli* with zones of inhibition 13 mm and activity index of 54.2% and compound HL_2 also showed moderate activity with zone 16 mm and activity index of 72.7 % (**Table 12**).

Compounds HL_1 , HL_2 , HL_3 and complex (1) exhibited antifungal activity against *C. albicans* with inhibition zones of 4,11,13 and 7 mm and activity index of 15.4%,42.3% 50% and 26.9%, respectively. By investigating the variation in the antimicrobial activities of the tested compounds it was revealed that the presence of Cl, NO_2 in some compounds such as HL_3

and HL_4 may be result moderate activities against tested microorganisms when compared with standard compounds.

3.11.3. Cytotoxic

In view of the biological activity of azo dye complexes, we firstly evaluated the ability of 3-aminophenol derivatives to inhibit cancer cell growth against Hepatocellular carcinoma liver (HCC). In our experiments, half maximal inhibitory concentration (IC_{50}) values (compound concentration that produces 50% of cell death) were calculated. For comparison purposes the cytotoxicity of Fluorouracil (5-FU) and the free ligand as well as the metal complexes was evaluated under the same experimental conditions. The IC_{50} of the complexes are higher than that of ligands, and there is no synergist effect with the complexation with the metal. A slight decrease of IC_{50} is observed only for the $[Cu(L_1)(OAc)]H_2O$ complex against MCF-7. Therefore, the chelation of the free ligand with metal ion is essential for anticancer activities of these complexes. Importantly, it should be emphasized that Cu(II) complexes exhibits considerable cell growth inhibition activity against human liver hepatocellular carcinoma HepG2 cells similar to that of 5-FU (7.9 lg/ml) for HePG2. These gratifying results are encouraging its further screening in *vitro*. Therefore, its further biological evaluation in *vitro* as well as studies of mechanism of action is necessary.

Cytotoxic and antitumor activity of ligands (HL_n) and its metal complexes were tested against (HePG2) and MCF-7cell line was detected by using different concentrations of the tested compounds (1.56, 3.125, 6.25,12.5, 25,50 1.56 µg/ml) and viability cells (%) were determined by the colorimetric method [59,60].

The results revealed that all tested compounds have cytotoxic and antitumor activity against the breast carcinoma cell line. HL_2 ,HL_3 ligands and complex (1) were found to exhibit potent anticancer activity which have better activity than complex (4). In **Table 13** values of IC_{50} decrease activity of compounds increased against the tumor and we can apply as anti-tumors drugs against tumors. The results shown in **Fig. S10 and Fig. 11** revealed that all tested compounds have cytotoxic and antitumor activity against the breast carcinoma cell line and human liver hepatocellular carcinoma with superiority.

***3.12.* DNA binding studies**

Absorption titration studies is one of the most universally methods used to study the binding modes linking DNA compounds [61,62]. The phenolic -OH group of the ligands may enhance their affinity towards DNA binding through formation of hydrogen bonding. Absorption titration experiments were performed with fixed concentrations of the ligands HL_n and Cu(II) complexes (**1**-**4**) (40 µM) while gradually increasing concentration of DNA in 25 °C at 442, 488, 439 and 453 nm for the ligands (HL_n), respectively and 466, 453, 454

and 456 nm for Cu(II) complexes (**1-4**), respectively. The absorption spectra of these ligands and Cu(II) complexes with increasing concentration of CT-DNA in the range 300-600 nm are shown in **Fig. S11 and Fig. 12**, respectively.

Upon the addition of increasing amount of CT-DNA, a significant hyperchromic effect was observed accompanied by a moderate red shift of 2–3 nm, indicative of stabilization of the DNA helix. These spectral characteristic suggest that the ligands and complexes bind either to the external contact electrostatic binding or to the major and minor grooves of DNA. Moreover, this hyperchromic effect can be explained on the basis of these two phenomena. The intrinsic binding constants (K_b) of all the ligands (HL_n) and Cu(II) complexes (**1-4**) with CT-DNA were determined using Eq. 2 [63].

The values of K_b obtained from the absorption spectral technique for ligands (HL_n) were calculated as 2.68×10^5, 3.05×10^5, 3.52×10^5 and 4.62×10^5 M^{-1}, respectively. The K_b values obtained from the absorption spectral technique for Cu(II) complexes (**1-4**) were calculated as 3.06×10^5, 4.85×10^5, 5.97×10^5 and $8.62\ x10^5$ M^{-1}, respectively. The binding constant of the complexes (**1-4**) are comparatively higher than that of the ligands (HL_n) due to formats six ring. The higher values of the binding constant of the ligands HL_4 and HL_3 are due to the presence of electron withdrawing group NO_2 and Cl, respectively, as shown in **Fig. 13**.

Conclusions

The structures of Cu (II) complexes of the ligands (HL_n) were confirmed by elemental analyses, IR, ^{1}H- NMR, X-ray, molar conductance, mass spectra and thermal analysis data. It was found that the electron density on azo dye group decrease the bending of our ligands with the receptor (2a91) increase, ($HL_4 > HL_3 > HL_2 > HL_1$) and the results confirmed also that, the azo dye ligands derived from 3-aminophenol is efficient inhibitor of 2a91. The comparison of cytotoxicity indicated that the complexes (1) and (3) showed much lower IC_{50} values for HePG2 with cell line and also complexes (1) and (2) lower IC_{50} values for MCF-7 as well as HL_2, HL_3 ligands and complex (1) were found to exhibit potent anticancer activity which have better activity than complex (4). By comparing the results obtained of ABTS antioxidant activity of the azo ligand compounds reported in this study compounds HL_1, HL_2 , HL_3 and complex (1) and found that copper complex of ligand HL_1 is the only complex which increase the antioxidant activity than its ligand and the binding constant of the complexes (**1-4**) are comparatively higher than that of the ligands (HL_n) due to formats six ring. The higher values of the binding constant of the ligands HL_4 and HL_3 are due to the presence of electron withdrawing groups. Catalytic oxidation of alcohols to the corresponding aldehydes using Cu complexes was studied. The synthesized compounds have antibacterial activity against the Gram-positive bacteria: *Staphylococcus aureus* and

also against the Gram-negative bacteria: *Escherichia coli* and *Candida albicans* and this is may be due to the presence of electron withdrawing groups (NO_2 and Cl).

Acknowledgement

The authors would like to thank Prof. Dr. M.I. Abou-Dobara, Botany Department, Faculty of Science, Damietta University, Egypt for his help during testing antimicrobial activity.

Appendix A: Supplementary material

See the attached file.

References

[1] S. Yin, H Xu, W. Shi, Y. Gao, Y. Song, J. W. Y. Lam and B. Z. Tang, J. Polym., 46, 7670 (2005).

[2] Y. Nabeshima, A. Shishido, A. Kanazawa, T. Shiono, T. Ikeda and T. Hiyama, Chem. Mater., 9, 1480 (1997).

[3] T. Pooja and C. Malay, Indian J. Eng. Mater. Sci. , 11, 499 (2004).

[4] T.M. Robert, N.B. Robert and S.K. Bhattacharjee, Organic Chem. 6th Ed, New Delhi, Pearson Prentice Hall, 1096 (2011).

[5] H. Zollinger;"Color Chemistry Syntheses, Properties, Application of Organic Dyes and Pigments". 3rd Edition. Wiley-VCH (2003).

[6] L. Savanni, L. Chiasserini, A. Gaeta and C. Pellerano, Bioorg. Med. Chem., 10, 2193 (2002).

[7] A.Z. El-Sonbati, A.A.M. Belal, M.S. El-Gharib, Sh.M. Morgan, Spectrochim. Acta A 95, 627 (2012).

[8] A.Z. El-Sonbati, M.A. Diab, Sh.M. Morgan, J. Mol. Liq. 225, 195 (2017).

[9] M. Badea, R. Olar, E. Cristurean, D. Marinescu, A. Emandi, P. Budrugeac and E. Segal,. J. Therm. Anal. Calor., 77, 815 (2004).

[10] S.O. Podunavac-Kuzmanović, V.M. Leovac, G.S. Ćetkovi and S.L. Markov, Acta Periodica Techn., 33, 151 (2002).

[11] S. O. Podunavac-Kuzmanović and LJS. Vojinović, Acta Periodica Tech., 34, 119 (2003).

[12] A.Z. El-Sonbati, M.A. Diab, A.A.M. Belal, Sh.M. Morgan, Spectrochim. Acta A 99, 353 (2012).

[13] C.H. Ng, H.K.A. Ong, C.W. Kong, K.W. Tan, R. Rahman, B.M.Yamin, and S.W.Ng, Polyhedron, 25, 3118 (2006).

[14] M.J. Waring , J. Mol. Biol , 13, 269 (1965).

[15] M.F. Reichmann, C.A. Rice, C.A. Thomos and P. Doty, J. Am. Chem. Soc., 76 , 3047 (1954).

[16] A. Wolfe, G.H. Shimer and T. Meehan, Biochem., 26, 6392 (1987).

[17] A.B.A. El-Gazar, A.M.S. Youssef, M.M. Youssef, A.A. Abu-Hashem and F.A. Badria. Eur. J. Med. Chem., 44, 609 (2009).

[18] H.J. Mauceri, N. N. Hanna, M.A. Beckett, D.H, Gorski, M. J Staba, K. A. Stellato, K.Bigelow, R . Heimann, S . Gately, M. Dhanabal, G.A. Soff, V.P. Sukhatme, D.W Kufe and R. R, Weichselbaum, Nature, 394, 287 (1998) .

[19] Z. Bikadi and E. Hazai. J. Chem. Inf., 1, 15(2009).

[20] T. A. H. Merck, J. Comp. Chem.,17, 490 (1998).

[21] G. M. Morris and D. S. Goodsell, J. Comp. Chem., 19, 1639(1998).

[22] H.M. Refaat, H.A. El-Badway, Sh.M. Morgan, J. Mol. Liq. 220, 802 (2016).

[23] N.A. El-Ghamaz, A.Z. El-Sonbati, Sh.M. Morgan, J. Mol. Struc. 1027, 92 (2012).

[24] G.G. Mohamed, A.A. El-Sherif, M.A. Saad, S.E.A. El-Sawy, Sh.M. Morgan, J. Mol. Liq. 223 (2016) 1311–1332.

[25] M.I. Abou-Dobara, A.Z. El-Sonbati, Sh.M. Morgan, World J. Microbiol. Biotechnol. 29, 119 (2013).

[26] A.Z. El-Sonbati, M.A. Diab, M.M. El-Halawany, N.E. Salam, Spectrochim. Acta A 77, 755 (2010).

[27] K. Nakamoto, " Infrared and Raman Spectra of Inorganic and Coordination Compounds: Applications in Coordination Organometallic and Bioinorganic Chemistry " Part B, John Wiley and Sons, pp 59-62 (1997).

[28] R. Shirley, The CRYSFIRE System for Automatic Powder Indexing: User's Manual, The Lattice Press, Guildford, Surrey GU2 7NL, England, (2000).

[29] J. Laugier and B. Bochu, LMGP-suite suite of programs for the interpretation of X-ray experiments, ENSP/Laboratoire des Materiaux et du Genie Physique, B P 46.38042, Saint Martin d'Heres, France, (2000).

[30] W. Coats and J.P. Redfern, Nature, 20, 68 (1964).

[31] H.W. Horowitz and G. Metzger, Anal. Chem. 35, 1464 (1963).

[32] Z . Mitri, T . Constantine and R . O'Regan, Chem. Res. Pra., 2012 (2012), Article ID 743193.

[33] M.M. Ibrahim, A.M. Ramadan, G.A.M. Mersal and S.A. El-Shazly. J. Mol. Struct., 998, 1 (2011).

[34] A. Sreekanth and M. R. P Kurup. Polyhedron, 22 , 3321 (2003).

[35] F. A. Cotton and G .Wilkinson. Advanced Inorganic Chemistry. New Delhi, India: Wiley Eastern (Pvt) (1969).

[36] K. Singh, M.S. Barawa and P. Tyagi, Eur. J. Med. Chem., 42, 394 (2007).

[37] M. Gaber, S.A. El-Daly and Y.S.Y. El-Sayed. J. Mol. Struct., 922, 51 (2009).

[38] F.A. Cotton and G. Wilkinson, "Advanced Inorganic Chemistry", A Comprehensive Text. 4 th Ed., John Wiley and Sons, New York (1986).

[39] B.J. Hathaway and D.E. Billing, Coord. Chem. Rev.,5, 81 (1970).

[40] H. Montgomery and E.C. Lingefetter, Acta Cryst., 20, 628 (1966).

[41] C.J. Carrano, C.M. Nunn, R. Quan, J.A. Bomadies and V.I. Pecoran, Inorg. Chem., 29, 944 (1990).

[42] D. Kilveson, J. Chem. Phys., 8, 8631 (1997).

[43] M. Salavati-Niasari and F. Davar, Inorg. Chem. Commun., 9 , 304 (2006).

[44] J. Piera and J.E. Backvall, Angew. Chem. Int. Ed., 47, 3506 (2008).

[45] T. Chattopadhyay, M. Kogiso, M. Asakawa, T. Shimizu and M. Aoyagi, Catal. Commun., 12 , 9 (2010).

[46] D. Ramakrishna and B.R. Bhat, Inorg. Chem. Commun., 14, 690 (2011)

[47] C. Parmeggiani and F. Cardona, Green Chem., 14, 547 (2012).

[48] J.E. Steves and S.S. Stahl, J. Am. Chem. Soc. 135, 15742 (2013).

[49] D. Ramakrishna and B.R. Bhat, Inorg. Chem. Commun.,14, 690 (2011).

[50] A. Rezaeifard, M. Jafarpour, A. Naeimi and M. Salimi, Inorg. Chem. Commun., 15, 230 (2012).

[51] M.F. Semmelhack, C.R. Schmid, D.A. Cortes and C.S. Chou, J. Am. Chem. Soc., 106, 3374 (1984).

[52] L. Liu, J.L. Yan and W.Y. Yang, Catal. Commun., 9, 1379 (2008).

[53] B.Z. Zhan and A. Thompson, Tetrahedron , 6, 2917(2004).

[54] G. Ragagnin, B. Betemeier, S. Quici and P. Knochel, Tetrahedron, 58., 3985 (2002).

[55] P. Gamez, I.W.C.E. Arends, J. Reedijk and R.A. Sheldon, Chem. Commun., 2414 (2003).

[56] (a) N. Jiang and A.J. Ragauskas, Org. Lett., 7, 3689 (2005) .

(b) S. Striegler, Tetrahedron, 62 , 9109 (2006).

(c) S. Mannam, S.K. Alamsetti and G. Sekar, Adv. Synth. Catal., 349, 2253 (2007).

[57] A. K. Sadana, Y. Mirza, K. R. Aneja, and O. Prakash, Eur. J. Med. Chem., 38, 533 (2003).

[58] M.O. Agwara, P. T. Ndifon, N. B. Ndosiri, A. G. Paboudam, D. M. Yufanyi, and A. Mohamadou, Bull. Chem. Soc. Ethiopia, 24, 383 (2010).

[59] T. Mosmann, J. Immunol. Methods, 65, 55 (1983).

[60] P. Vijayan, G. Raghu, G. Ashok, S.A. Dhanaraj and B. Suresh, Indian J. Med. Res., 120, 24 (2004).

[61] M. S. Donnenberg , T. S. Whittam and E. coli, J. Clin. Invest., 107 , 539 (2001).

[62] L. Shivakumar, K. Shivaprasad and H. D. Revanasiddappa, Spectrochim. Acta A107, 203 (2013).

[63] C. Icsel, V.T. Yilmaz, F. Ari, E.Ulukaya and W.T.A. Harrison, Eur. J. Med. Chem. 60386 (2013).

Table 1. Physical properties and elemental analysis data of Cu(II) complexes (**1-4**).

Compound	Yield %	M.p. ^{o}C	Exp. (Calc.) %		
			C	H	N
[Cu (L_1)(OAc)] H_2O (1)	70	235	48.98 (49.11)	3.89 (4.09)	11.23 (11.46)
[Cu (L_2)(OAc)] H_2O (2)	68	243	47.55 (47.65)	3.43 (3.69)	11.63 (11.91)
[Cu (L_3)(OAc)] H_2O (3)	64	260	43.23 (43.41)	2.89 (3.10)	10.65 (10.85)
[Cu (L_4)(OAc)] H_2O (4)	84	>300	42.07 (42.26)	2.88 (3.02)	13.69 (14.09)

Table 2. Crystal data for complexes (1 and 4)

Complex	(1)	(4)
Space group	p2	p21
Crystal System	triclinic	monoclinic
Unit-cell dimensions		
a Å	16.5670	20.2460
b Å	11.1560	18.8100
c Å	8.4430	15.1780
α °	93.99	90.00
β °	98.22	99.88
γ °	89.43	90.00

Table 3. Thermal analysis data of Cu II) complexes**.**

Complex[a]	Temperature range (°C) Cu	TG weight loss % Found (Calc.)	Assignments
1	30-140	4.79 (4.91)	Outer H_2O molecule
	140-314	17.65 (16.09)	CH_3COO
	314-800	30.44 (32.46)	$C_7H_7N_2$
	>800	47.16 (46.79)	C_6H_6N + CuO
2	30-424	21.94 (21.84)	Outer H_2O molecule + CH_3COO
	424-800	30.92 (29.78)	$C_6H_5N_2$
	> 800	47.08 (48.64)	C_6H_6N + CuO
3	30-109	3.26 (4.65)	Outer H_2O molecule
	109-397	16.29 (15.24)	CH_3COO
	397-795	49.59 (49.74)	$C_9H_7N_3Cl$
	>795	30.84 (30.61)	C_3H_3 + CuO
4	30-251	7.07 (4.52)	Outer H_2O molecule
	251-377	20.68 (22.39)	CH_3CO+ NO_2
	377-800	24.31 (22.64)	C_6H_4N
	>800	48.02 (50.69)	$C_6H_5N_2O$ + CuO

[a] Numbers as given in Table 1.

Table 4. The thermodynamic activation parameters of decomposition processes of the ligands and their Cu(II) complexes[a].

Compound	Temp. range (^{o}C)	Method	Parameter					Correlation coefficient (r)
			E_a (kJ mol^{-1})	A (s^{-1})	-ΔS* (J mol^{-1} K^{-1})	ΔH* (kJ mol^{-1})	ΔG* (kJ mol^{-1})	
HL_1	140-342	CR HM	81.4 89.9	8.02X10^{5} 1.38x10^{7}	136 x10^{-3} 113 x10^{-3}	77.1 85.6	1.47 x10^{2} 1.44 x10^{2}	0.95338 0.92419
	342-806	CR HM	40.8 46.8	236 x10^{-3} 14.9 x10^{2}	266 x10^{-3} 250 x10^{-3}	33.7 39.7	2.59 ×10^{2} 2.52 ×10^{2}	0.99916 0.99932
HL_2	124-298	CR HM	81.42 91.3	2.24x10^{6} 7.94x10^{7}	1.27 x10^{-3} 9.77 x10^{-4}	78 87.3	1.40 x10^{2} 1.35 x10^{2}	0.98318 0.96551
	298-802	CR HM	21.8 29.9	2.55 x10^{-3} 104 x10^{-3}	284 x10^{-3} 2.72 x10^{-3}	15 23	2.49 x10^{2} 2.47 x10^{2}	0.9999 0.99959
HL_3	86-312	CR HM	65.7 72.4	5.32x10^{3} 9.91x10^{5}	1.77 x10^{-3} 1.34 x10^{-3}	61.7 68.5	1.46 x10^{2} 1.32 x10^{2}	0.99158 0.98151
	312-803	CR HM	25.8 36.3	2.10x10^{3} 3 x10^{-1}	1.90 x10^{-3} 2.63 x10^{-3}	18.9 29.4	1.77 x10^{2} 2.48x10^{2}	0.99831 0.99289
HL_4	119-172	CR HM	111 131	1.98x10^{12} 5.52x10^{14}	1.23 x10^{2} 3.45 x10^{2}	107 128	1.12 x10^{2} 1.13 x10^{2}	0.99717 0.97945
	172-355	CR HM	77.1 86.7	8.68x10^{4} 2.48x10^{6}	1.55 x10^{2} 1.27 x10^{2}	72.6 82.2	1.56 x10^{2} 1.51 x10^{2}	0.999 0.99472
1	140-205	CR HM	90.1 96.3	2.93x10^{8} 2.78 x10^{9}	8.62 x10^{2} 6.75 x10^{2}	86.4 92.6	1.25 x10^{2} 1.23 x10^{2}	0.98087 0.97456
	205-252	CR HM	195 195	2.21 x10^{18} 4.09 x10^{18}	1.02 x10^{2} 1.07 x10^{2}	191 190	1.40 x10^{2} 1.37 x10^{2}	0.9886 0.9946
2	153-281	CR HM	58.3 66.3	4.88 x10^{3} 9.52 x10^{4}	1.78 x10^{2} 1.54 x10^{2}	54.2 62.2	1.42 x10^{2} 1.38 x10^{2}	0.99724 0.98846
	282-424	CR HM	75.5 85.5	7.37x10^{3} 8.87 x10^{4}	1.77 x10^{2} 1.56 x10^{2}	70.3 80.3	1.81 x10^{2} 1.78 x10^{2}	0.98731 0.97902
3	110-237	CR HM	32.2 42.2	1.81 x10^{2} 6.94 x10^{2}	2.45 x10^{2} 2.14 x10^{2}	27.8 37.8	1.57 x10^{2} 1.51 x10^{2}	0.99768 0.99126
	237-795	CR HM	50.9 66.1	129 x10^{2} 2.44 x10^{2}	2.52 x10^{2} 2.27 x10^{2}	43.7 58.9	2.63 x10^{2} 2.57 x10^{2}	0.99003 0.98077
4	149-251	CR HM	60.6 69.3	1.66 x10^{4} 4.08 x10^{5}	1.68 x10^{2} 1.41 x10^{2}	56.7 65.4	1.36 x10^{2} 1.32 x10^{2}	0.98038 0.98361
	251-306	CR HM	181 191	1.05 x10^{15} 2.41 x10^{16}	3.75 x10^{2} 6.36 x 10^{2}	176 187	1.55 x10^{2} 1.52 x10^{2}	0.98253 0.98304

[a]Numbers as given in Table 1.

Table 5. Selected geometric parameters for complex **(1)**.

Bond lengths (Å)		Bond angles (°)	
C(22)-H(37)	1.115	H(37)-C(22)-H(36)	102.932
C(22)-H(36)	1.116	H(37)-C(22)-H(35)	102.878
C(22)-H(35)	1.116	H(37)-C(22)-C(20)	103.558
C(17)-H(34)	1.114	H(36)-C(22)-H(35)	112.767
C(17)-H(33)	1.113	H(36)-C(22)-C(20)	116.185
C(17)-H(32)	1.114	H(35)-C(22)-C(20)	116.037
C(16)-H(31)	1.105	C(22)-C(20)-O(21)	166.695
C(15)-H(30)	1.103	C(22)-C(20)-O(19)	78.599
C(13)-H(29)	1.103	O(21)-C(20)-O(19)	88.097
C(12)-H(28)	1.104	H(34)-C(17)-H(33)	107.859
N(7)-H(27)	1.049	H(34)-C(17)-H(32)	108.471
N(7)-H(26)	1.049	H(34)-C(17)-C(14)	110.001
C(5)-H(25)	1.104	H(33)-C(17)-H(32)	107.168
C(2)-H(24)	1.104	H(33)-C(17)-C(14)	112.506
C(1)-H(23)	1.103	H(32)-C(17)-C(14)	110.692
C(9)-C(16)	1.353	H(30)-C(15)-C(16)	119.197
C(15)-C(16)	1.342	H(30)-C(15)-C(14)	119.854
C(14)-C(15)	1.343	C(16)-C(15)-C(14)	120.948
C(13)-C(14)	1.343	C(15)-C(14)-C(13)	117.732
C(12)-C(13)	1.342	C(15)-C(14)-C(17)	121.702
C(9)-C(12)	1.353	C(13)-C(14)-C(17)	120.566
O(21)-Cu(18)	1.812	H(29)-C(13)-C(14)	119.401
O(19)-Cu(18)	1.806	H(29)-C(13)-C(12)	119.441
C(20)-C(22)	1.534	C(14)-C(13)-C(12)	121.158
C(20)-O(21)	1.246	H(31)-C(16)-C(9)	120.364
O(19)-C(20)	1.581	H(31)-C(16)-C(15)	117.479
N(10)-Cu(18)	1.315	C(9)-C(16)-C(15)	122.156
O(8)-Cu(18)	1.804	H(28)-C(12)-C(13)	117.038
C(14)-C(17)	1.51	H(28)-C(12)-C(9)	121.005
N(11)-C(3)	1.276	C(13)-C(12)-C(9)	121.95
N(10)-N(11)	1.272	Cu(18)-O(21)-C(20)	109.607
C(9)-N(10)	1.282	Cu(18)-O(19)-C(20)	95.938
C(4)-O(8)	1.37	O(21)-Cu(18)-O(19)	66.357
C(6)-N(7)	1.268	O(21)-Cu(18)-N(10)	121.366
C(6)-C(1)	1.341	O(21)-Cu(18)-O(8)	118.765
C(5)-C(6)	1.342	O(19)-Cu(18)-N(10)	117.501
C(4)-C(5)	1.347	O(19)-Cu(18)-O(8)	115.706
C(3)-C(4)	1.353	N(10)-Cu(18)-O(8)	110.646
C(2)-C(3)	1.346	C(16)-C(9)-C(12)	116.034
C(1)-C(2)	1.341	C(16)-C(9)-N(10)	120.465
		C(12)-C(9)-N(10)	123.47
		Cu(18)-N(10)-N(11)	112.469
		Cu(18)-N(10)-C(9)	115.689
		N(11)-N(10)-C(9)	114.831
		H(27)-N(7)-H(26)	119.653
		H(27)-N(7)-C(6)	120.166
		H(26)-N(7)-C(6)	120.182
		N(7)-C(6)-C(1)	120.193
		N(7)-C(6)-C(5)	120.387
		C(1)-C(6)-C(5)	119.417
		Cu(18)-O(8)-C(4)	105.712

	H(25)-C(5)-C(6)	119.66
	H(25)-C(5)-C(4)	118.323
	C(6)-C(5)-C(4)	122.015
	C(3)-N(11)-N(10)	126.372
	O(8)-C(4)-C(5)	119.785
	O(8)-C(4)-C(3)	122.116
	C(5)-C(4)-C(3)	118.072
	N(11)-C(3)-C(4)	122.521
	N(11)-C(3)-C(2)	117.543
	C(4)-C(3)-C(2)	119.927
	H(24)-C(2)-C(3)	120.366
	H(24)-C(2)-C(1)	118.547
	C(3)-C(2)-C(1)	121.084
	H(23)-C(1)-C(6)	120.837
	H(23)-C(1)-C(2)	119.697
	C(6)-C(1)-C(2)	119.466

Table 6. Selected geometric parameters for complex **(2)**.

Bond lengths (Å)		Bond angles (°)	
C(21)-H(34)	1.115	H(34)-C(21)-H(33)	102.884
C(21)-H(33)	1.116	H(34)-C(21)-H(32)	102.93
C(21)-H(32)	1.116	H(34)-C(21)-C(19)	103.568
C(16)-H(31)	1.104	H(33)-C(21)-H(32)	112.759
C(15)-H(30)	1.103	H(33)-C(21)-C(19)	116.054
C(14)-H(29)	1.103	H(32)-C(21)-C(19)	116.165
C(13)-H(28)	1.103	C(21)-C(19)-O(20)	166.692
C(12)-H(27)	1.105	C(21)-C(19)-O(18)	78.594
N(7)-H(26)	1.049	O(20)-C(19)-O(18)	88.098
N(7)-H(25)	1.049	H(30)-C(15)-C(16)	120.055
C(5)-H(24)	1.104	H(30)-C(15)-C(14)	119.71
C(2)-H(23)	1.104	C(16)-C(15)-C(14)	120.235
C(1)-H(22)	1.103	H(29)-C(14)-C(15)	120.42
C(9)-C(16)	1.354	H(29)-C(14)-C(13)	120.4
C(15)-C(16)	1.342	C(15)-C(14)-C(13)	119.178
C(14)-C(15)	1.34	H(28)-C(13)-C(14)	119.798
C(13)-C(14)	1.34	H(28)-C(13)-C(12)	120.092
C(12)-C(13)	1.342	C(14)-C(13)-C(12)	120.109
C(9)-C(12)	1.354	H(31)-C(16)-C(9)	121.038
O(20)-Cu(17)	1.812	H(31)-C(16)-C(15)	116.964
O(18)-Cu(17)	1.806	C(9)-C(16)-C(15)	121.992
C(19)-C(21)	1.534	H(27)-C(12)-C(13)	117.416
C(19)-O(20)	1.246	H(27)-C(12)-C(9)	120.458
O(18)-C(19)	1.581	C(13)-C(12)-C(9)	122.125
N(10)-Cu(17)	1.315	Cu(17)-O(20)-C(19)	109.608
O(8)-Cu(17)	1.804	Cu(17)-O(18)-C(19)	95.937
N(11)-C(3)	1.276	O(20)-Cu(17)-O(18)	66.357
N(10)-N(11)	1.272	O(20)-Cu(17)-N(10)	121.518
C(9)-N(10)	1.283	O(20)-Cu(17)-O(8)	118.968
C(4)-O(8)	1.37	O(18)-Cu(17)-N(10)	117.426
C(6)-N(7)	1.268	O(18)-Cu(17)-O(8)	115.497
C(6)-C(1)	1.341	N(10)-Cu(17)-O(8)	110.553
C(5)-C(6)	1.342	C(16)-C(9)-C(12)	116.339
C(4)-C(5)	1.347	C(16)-C(9)-N(10)	123.359
C(3)-C(4)	1.354	C(12)-C(9)-N(10)	120.27
C(2)-C(3)	1.346	Cu(17)-N(10)-N(11)	112.381
C(1)-C(2)	1.341	Cu(17)-N(10)-C(9)	115.713
		N(11)-N(10)-C(9)	114.911
		H(26)-N(7)-H(25)	119.644
		H(26)-N(7)-C(6)	120.165
		H(25)-N(7)-C(6)	120.191
		N(7)-C(6)-C(1)	120.206
		N(7)-C(6)-C(5)	120.37
		C(1)-C(6)-C(5)	119.421
		Cu(17)-O(8)-C(4)	105.642
		H(24)-C(5)-C(6)	119.666
		H(24)-C(5)-C(4)	118.319
		C(6)-C(5)-C(4)	122.012
		C(3)-N(11)-N(10)	126.329
		O(8)-C(4)-C(5)	119.779

	O(8)-C(4)-C(3)	122.12
	C(5)-C(4)-C(3)	118.073
	N(11)-C(3)-C(4)	122.503
	N(11)-C(3)-C(2)	117.562
	C(4)-C(3)-C(2)	119.926
	H(23)-C(2)-C(3)	120.365
	H(23)-C(2)-C(1)	118.549
	C(3)-C(2)-C(1)	121.083
	H(22)-C(1)-C(6)	120.836
	H(22)-C(1)-C(2)	119.698
	C(6)-C(1)-C(2)	119.466

Table 7. Selected geometric parameters for complex **(3)**.

Bond lengths (Å)		Bond angles (^{o})	
C(22)-H(34)	1.115	H(34)-C(22)-H(33)	102.89
C(22)-H(33)	1.116	H(34)-C(22)-H(32)	102.933
C(22)-H(32)	1.116	H(34)-C(22)-C(20)	103.571
C(16)-H(31)	1.104	H(33)-C(22)-H(32)	112.758
C(15)-H(30)	1.103	H(33)-C(22)-C(20)	116.067
C(13)-H(29)	1.103	H(32)-C(22)-C(20)	116.144
C(12)-H(28)	1.105	C(22)-C(20)-O(21)	166.69
N(7)-H(27)	1.049	C(22)-C(20)-O(19)	78.595
N(7)-H(26)	1.049	O(21)-C(20)-O(19)	88.095
C(5)-H(25)	1.104	H(30)-C(15)-C(16)	119.351
C(2)-H(24)	1.104	H(30)-C(15)-C(14)	120.549
C(1)-H(23)	1.103	C(16)-C(15)-C(14)	120.1
C(9)-C(16)	1.353	C(15)-C(14)-C(13)	119.331
C(15)-C(16)	1.342	C(15)-C(14)-Cl(17)	120.29
C(14)-C(15)	1.341	C(13)-C(14)-Cl(17)	120.378
C(13)-C(14)	1.341	H(29)-C(13)-C(14)	120.644
C(12)-C(13)	1.342	H(29)-C(13)-C(12)	119.416
C(9)-C(12)	1.354	C(14)-C(13)-C(12)	119.939
O(21)-Cu(18)	1.812	H(31)-C(16)-C(9)	120.956
O(19)-Cu(18)	1.806	H(31)-C(16)-C(15)	116.977
C(20)-C(22)	1.534	C(9)-C(16)-C(15)	122.061
C(20)-O(21)	1.246	H(28)-C(12)-C(13)	117.394
O(19)-C(20)	1.581	H(28)-C(12)-C(9)	120.377
N(10)-Cu(18)	1.315	C(13)-C(12)-C(9)	122.229
O(8)-Cu(18)	1.804	Cu(18)-O(21)-C(20)	109.609
C(14)-Cl(17)	1.726	Cu(18)-O(19)-C(20)	95.934
N(11)-C(3)	1.276	O(21)-Cu(18)-O(19)	66.353
N(10)-N(11)	1.272	O(21)-Cu(18)-N(10)	121.535
C(9)-N(10)	1.283	O(21)-Cu(18)-O(8)	119.302
C(4)-O(8)	1.371	O(19)-Cu(18)-N(10)	117.441
C(6)-N(7)	1.268	O(19)-Cu(18)-O(8)	115.25
C(6)-C(1)	1.341	N(10)-Cu(18)-O(8)	110.43
C(5)-C(6)	1.342	C(16)-C(9)-C(12)	116.318
C(4)-C(5)	1.347	C(16)-C(9)-N(10)	123.394
C(3)-C(4)	1.354	C(12)-C(9)-N(10)	120.256
C(2)-C(3)	1.346	Cu(18)-N(10)-N(11)	112.3
C(1)-C(2)	1.341	Cu(18)-N(10)-C(9)	115.66
		N(11)-N(10)-C(9)	115.033
		H(27)-N(7)-H(26)	119.643
		H(27)-N(7)-C(6)	120.168
		H(26)-N(7)-C(6)	120.188
		N(7)-C(6)-C(1)	120.197
		N(7)-C(6)-C(5)	120.376
		C(1)-C(6)-C(5)	119.424
		Cu(18)-O(8)-C(4)	105.557
		H(25)-C(5)-C(6)	119.663
		H(25)-C(5)-C(4)	118.32
		C(6)-C(5)-C(4)	122.015
		C(3)-N(11)-N(10)	126.247
		O(8)-C(4)-C(5)	119.778

	O(8)-C(4)-C(3)	122.134
	C(5)-C(4)-C(3)	118.061
	N(11)-C(3)-C(4)	122.483
	N(11)-C(3)-C(2)	117.57
	C(4)-C(3)-C(2)	119.938
	H(24)-C(2)-C(3)	120.365
	H(24)-C(2)-C(1)	118.558
	C(3)-C(2)-C(1)	121.074
	H(23)-C(1)-C(6)	120.836
	H(23)-C(1)-C(2)	119.695
	C(6)-C(1)-C(2)	119.469

Table 8. Selected geometric parameters for complex **(4)**.

Bond lengths (Å)		Bond angles (°)	
C(21)-H(36)	1.115	H(36)-C(21)-H(35)	102.887
C(21)-H(35)	1.116	H(36)-C(21)-H(34)	102.938
C(21)-H(34)	1.116	H(36)-C(21)-C(19)	103.571
C(16)-H(33)	1.105	H(35)-C(21)-H(34)	112.764
C(15)-H(32)	1.104	H(35)-C(21)-C(19)	115.992
C(13)-H(31)	1.104	H(34)-C(21)-C(19)	116.212
C(12)-H(30)	1.105	C(21)-C(19)-O(20)	166.676
N(7)-H(29)	1.049	C(21)-C(19)-O(18)	78.602
N(7)-H(28)	1.049	O(20)-C(19)-O(18)	88.076
C(5)-H(27)	1.104	C(14)-N(22)-O(24)	123.214
C(2)-H(26)	1.104	C(14)-N(22)-O(23)	123
C(1)-H(25)	1.103	O(24)-N(22)-O(23)	113.783
C(9)-C(16)	1.352	H(32)-C(15)-C(16)	117.135
C(15)-C(16)	1.343	H(32)-C(15)-C(14)	121.05
C(14)-C(15)	1.347	C(16)-C(15)-C(14)	121.814
C(13)-C(14)	1.346	C(15)-C(14)-C(13)	116.425
C(12)-C(13)	1.343	C(15)-C(14)-N(22)	121.646
C(9)-C(12)	1.352	C(13)-C(14)-N(22)	121.929
O(20)-Cu(17)	1.812	H(31)-C(13)-C(14)	121.047
O(18)-Cu(17)	1.806	H(31)-C(13)-C(12)	117.29
C(19)-C(21)	1.534	C(14)-C(13)-C(12)	121.663
C(19)-O(20)	1.246	H(33)-C(16)-C(9)	120.722
O(18)-C(19)	1.581	H(33)-C(16)-C(15)	117.066
N(10)-Cu(17)	1.315	C(9)-C(16)-C(15)	122.202
O(8)-Cu(17)	1.804	H(30)-C(12)-C(13)	117.568
C(14)-N(22)	1.258	H(30)-C(12)-C(9)	120.088
N(11)-C(3)	1.276	C(13)-C(12)-C(9)	122.344
N(10)-N(11)	1.272	Cu(17)-O(20)-C(19)	109.61
C(9)-N(10)	1.283	Cu(17)-O(18)-C(19)	95.93
C(4)-O(8)	1.37	O(20)-Cu(17)-O(18)	66.366
C(6)-N(7)	1.267	O(20)-Cu(17)-N(10)	121.17
C(6)-C(1)	1.341	O(20)-Cu(17)-O(8)	118.263
C(5)-C(6)	1.341	O(18)-Cu(17)-N(10)	117.75
C(4)-C(5)	1.347	O(18)-Cu(17)-O(8)	116.576
C(3)-C(4)	1.353	N(10)-Cu(17)-O(8)	110.492
C(2)-C(3)	1.346	C(16)-C(9)-C(12)	115.522
C(1)-C(2)	1.341	C(16)-C(9)-N(10)	123.561
N(22)-O(24)	1.314	C(12)-C(9)-N(10)	120.888
N(22)-O(23)	1.314	Cu(17)-N(10)-N(11)	112.325
		Cu(17)-N(10)-C(9)	115.509
		N(11)-N(10)-C(9)	115.015
		H(29)-N(7)-H(28)	119.628
		H(29)-N(7)-C(6)	120.176
		H(28)-N(7)-C(6)	120.196
		N(7)-C(6)-C(1)	120.17
		N(7)-C(6)-C(5)	120.367
		C(1)-C(6)-C(5)	119.46
		Cu(17)-O(8)-C(4)	105.75
		H(27)-C(5)-C(6)	119.676
		H(27)-C(5)-C(4)	118.331

	C(6)-C(5)-C(4)	121.99
	C(3)-N(11)-N(10)	126.356
	O(8)-C(4)-C(5)	119.825
	O(8)-C(4)-C(3)	122.097
	C(5)-C(4)-C(3)	118.049
	N(11)-C(3)-C(4)	122.458
	N(11)-C(3)-C(2)	117.551
	C(4)-C(3)-C(2)	119.982
	H(26)-C(2)-C(3)	120.379
	H(26)-C(2)-C(1)	118.563
	C(3)-C(2)-C(1)	121.054
	H(25)-C(1)-C(6)	120.851
	H(25)-C(1)-C(2)	119.704
	C(6)-C(1)-C(2)	119.445

Table 9. Calculated quantum chemical properties for the ligands (HL_n) and their complexes[a].

Compound	E_{HOMO} (eV)	E_{LUMO} (eV)	ΔE (eV)	χ (eV)	η (eV)	σ $(eV)^{-1}$	Pi (eV)	S $(eV)^{-1}$	ω (eV)	ΔN_{max}
HL_1	-3.061	-1.841	1.220	2.451	0.610	1.639	-2.451	0.819	4.924	4.018
1	-5.002	-2.944	2.058	3.973	1.029	0.972	-3.973	0.486	7.670	3.861
HL_2	-3.218	-1.838	1.380	2.528	0.690	1.449	-2.528	0.725	4.631	3.664
2	-5.023	-2.947	2.076	3.985	1.038	0.963	-3.985	0.482	7.649	3.839
HL_3	-2.733	-1.836	0.890	2.285	0.450	2.229	-2.285	1.115	5.818	5.094
3	-4.968	-2.946	2.022	3.957	1.011	0.989	-3.957	0.495	7.744	3.914
HL_4	-5.479	-1.850	3.629	3.665	1.815	0.551	-3.665	0.276	3.700	2.020
4	-5.595	-4.502	1.093	5.049	0.547	1.830	-5.049	0.915	23.3189	9.238

[a]Numbers as given in Table 1.

Table 10. ESR spectral assignment for Cu(II) complexes (1-3)

complex[a]	g_{ll}	$g_{\perp}$	$g_{av.}$	G	α^2	β^2	$A_{ll}x10^{-4}$	f	K^2_{ll}	$K^2_{\perp}$	K^2
1	2.223	2.059	2..113	3.90	0.69	0.76	183	122	0.585	0.645	0.625
2	2.230	2.050	2.110	4.77	0.75	0.78	163	135	0.606	0.634	0.625
3	2.262	2.050	2.121	5.44	0.76	0.80	157	144	0.612	0.625	0.621

[a] Numbers as given in Table 1.

Table 11. ABTS antioxidant activity assay of the HL_n ligands and their Cu (II) complexes[a].

Compound	Absorbance of samples	inhibition (%)
Control of ABTS	0.520	0
Ascorbic-acid	0.057	89.0
HL_1	0.069	86.7
HL_2	0.056	89.2
HL_3	0.057	89.0
HL_4	0.110	78.8
1	0.067	87.1
2	0.333	36.0
3	0.334	35.8
4	0.383	26.3

[a]Numbers as given in Table 1.

Table 12. Antibacterial and antifungal activity data of the ligands (HL_n) and complexes [a].

Compound (mg\ml)	*E. coli*		*S. aureus*		*C. albicans*	
	Diameter of inhibition zone (mm)	% Activity index	Diameter of inhibition zone (mm)	% Activity index	Diameter of inhibition zone (mm)	% Activity index
HL_1	7	29.2	10	45.4	4	15.4
HL_2	11	45.8	16	72.7	11	42.3
HL_3	10	41.7	13	59.1	13	50.0
HL_4	2	8.3	8	36.4	-	-
1	13	54.2	12	54.5	7	26.9
2	-	-	6	27.3	-	-
3	-	-	3	13.6	-	-
4	-	-	-	-	-	-
Ampicillin	24	100	22	100	-	-
Colitrimazole	-	-	-	-	26	100

[a]Numbers as given in Table 1.

Table 13. Cytotoxic activity of HL_n ligand and their complexes[a] against human tumor cells.

Compound	In vitro Cytotoxicity IC_{50} (µg/ml)	
	HePG2	MCF-7
Fluorouracil (5-FU)	7.9±0.24	5.6±0.13
HL_1	11.0±0.94	19.7±1.18
HL_2	8.8±0.68	9.0±0.65
HL_3	9.7±0.76	13.5±1.34
HL_4	11.9±1.13	46.2±4.11
1	11.9±1.05	17.7±1.40
2	58.1±3.97	85.1±5.52
3	46.1±3.86	90.5±6.36
4	74.0±4.89	97.3±6.27

[a]Numbers as given in Table 1.

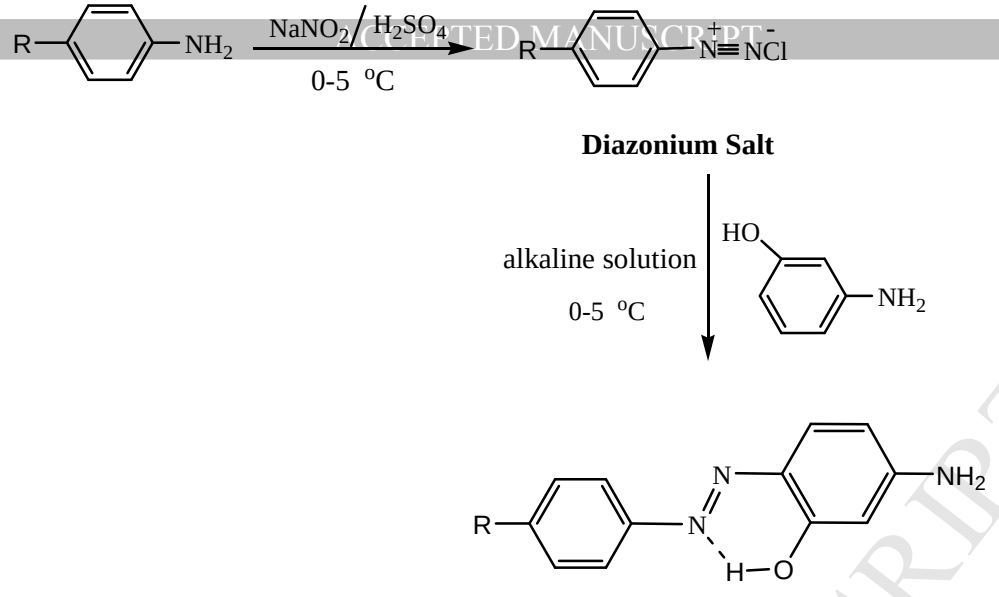

R= -CH_3 (HL_1), -H (HL_2), -Cl (HL_3) and –NO_2 (HL_4)

Fig. 1. Structures of the investigated ligands (**HL_n**).

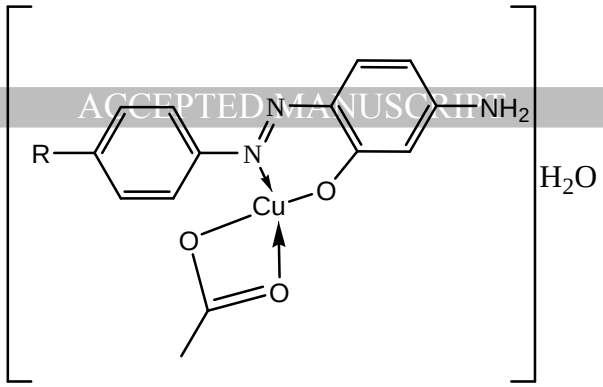

Fig. 2. Formation of the complex ligands.

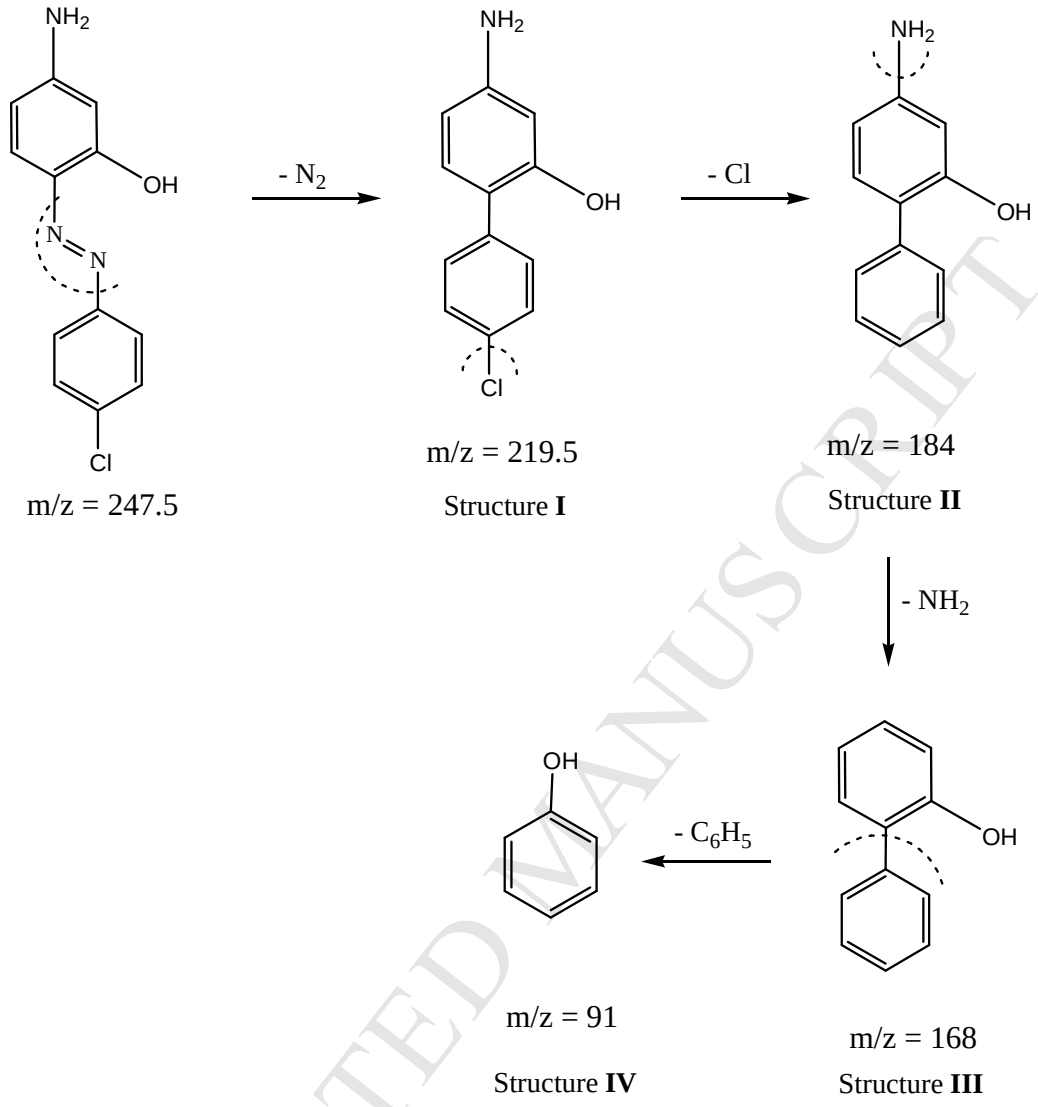

Fig. 3. Fragmentation patterns of HL_3 ligand.

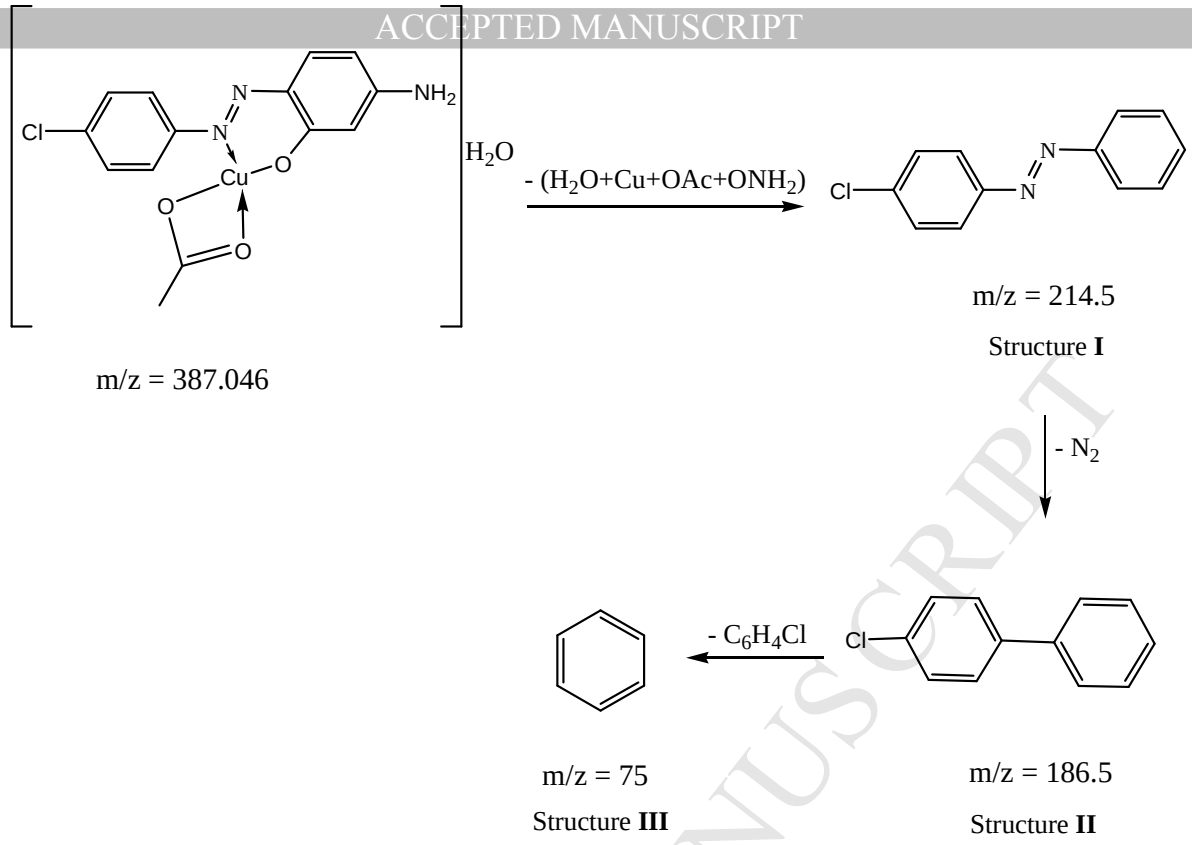

Fig. 4. Fragmentation patterns of $[Cu(L_3)(OAc)]H_2O$ complex.

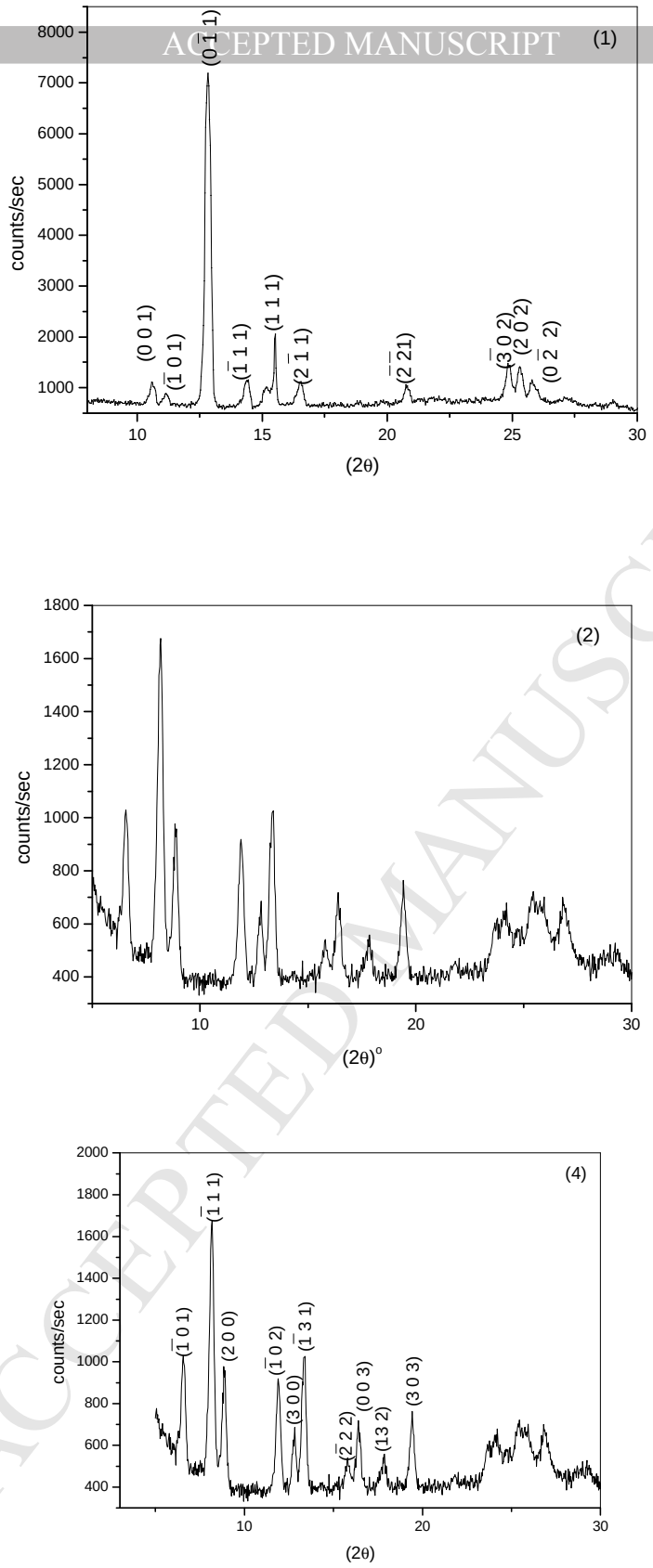

Fig. 5. The XRD diffraction patterns of complexes (1,2 and 4).

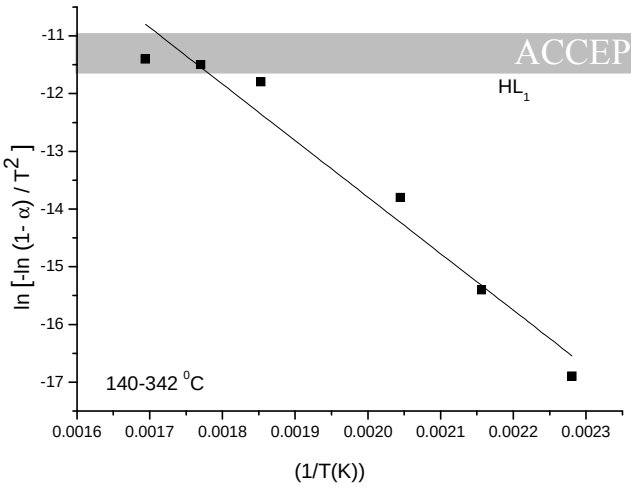

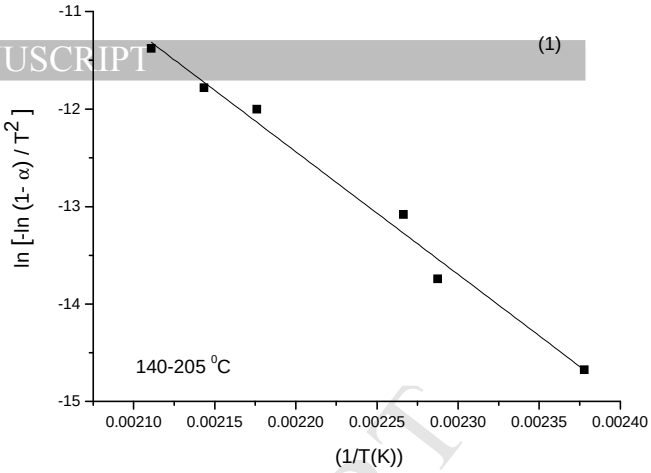

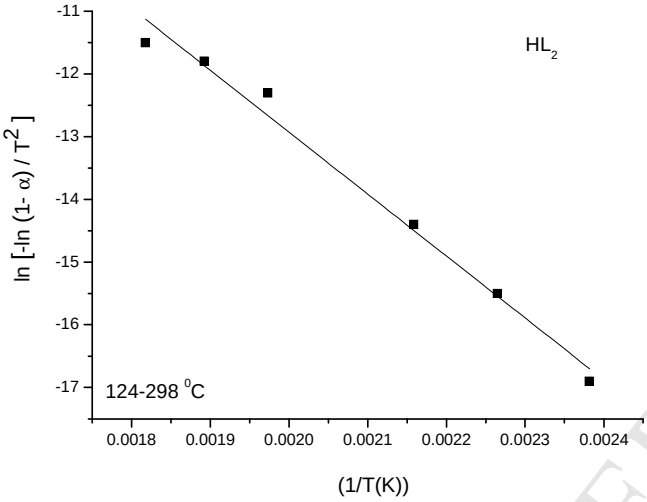

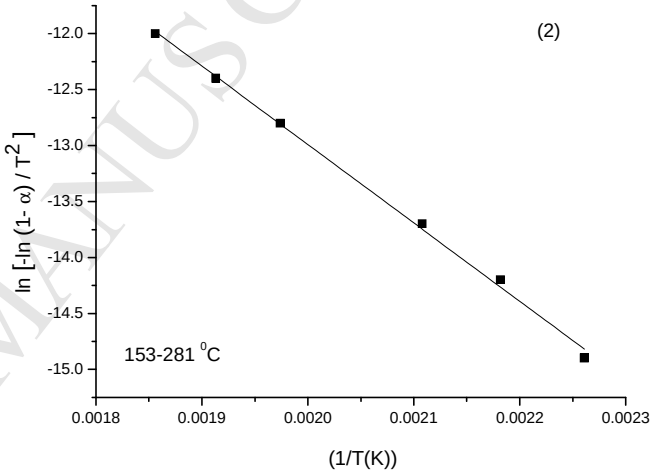

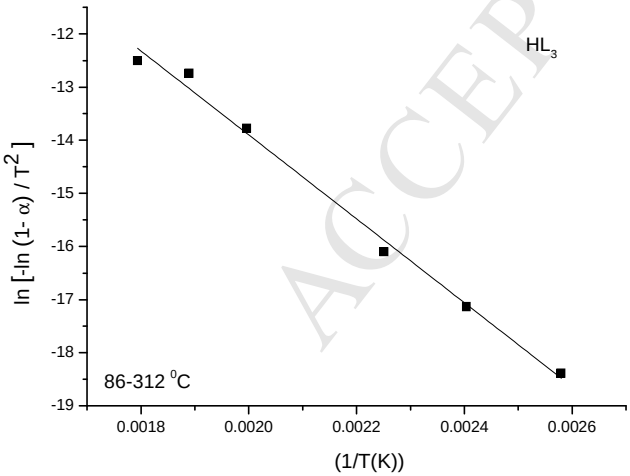

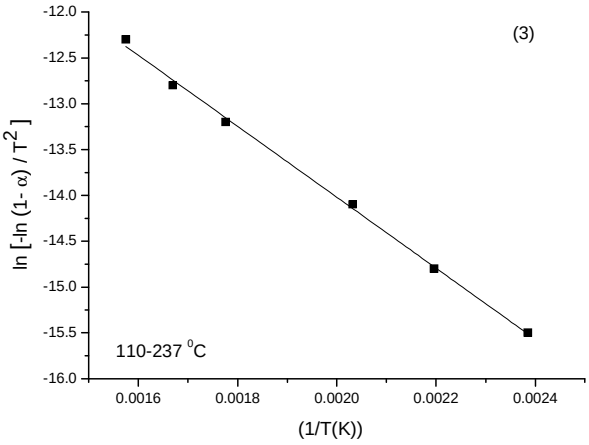

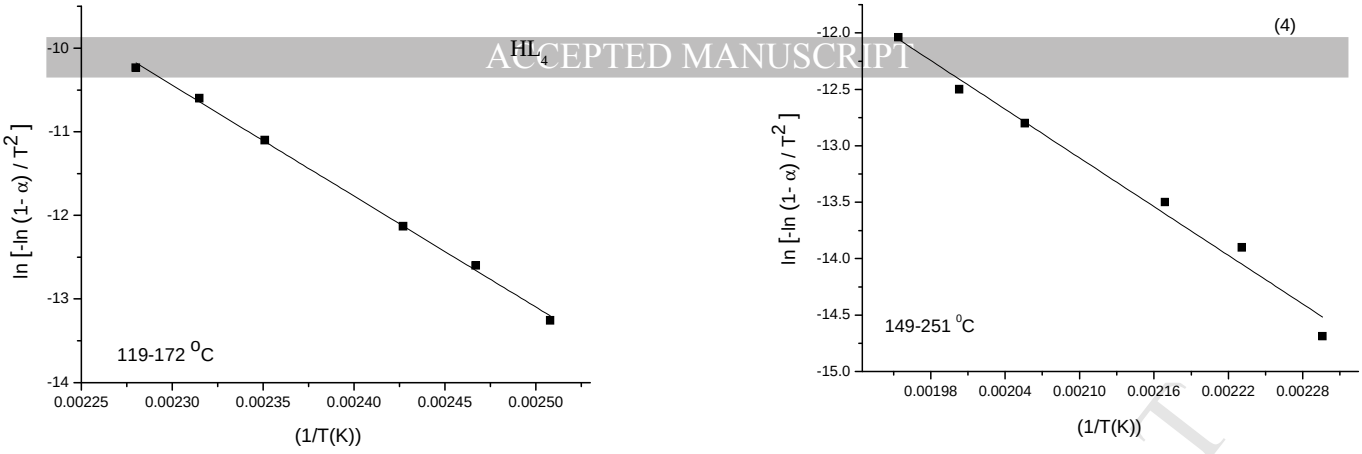

Fig. 6. Coats–Redfern (CR) of the ligands (**HL$_n$**) and their Cu(II) complexes (**1-4**).

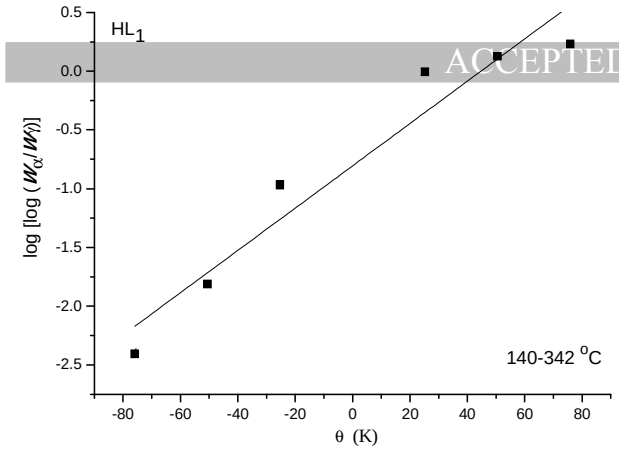

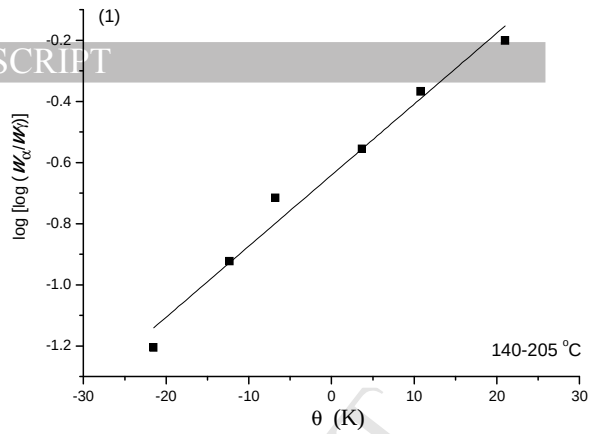

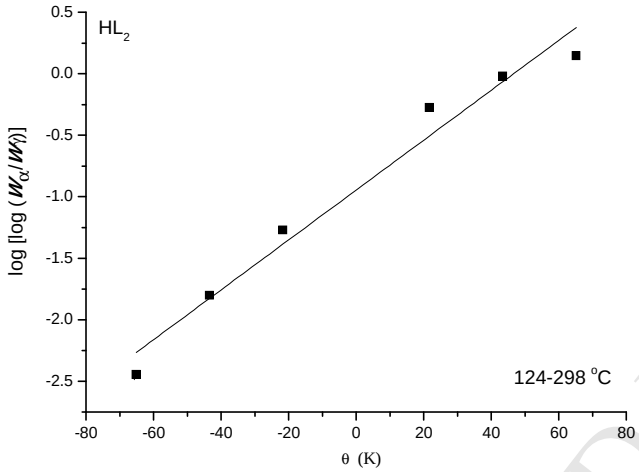

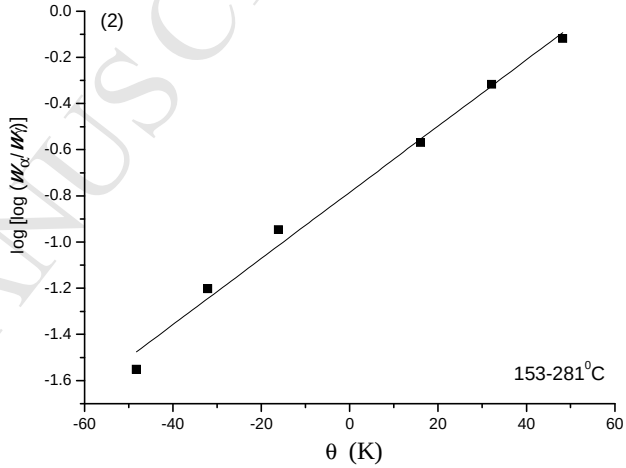

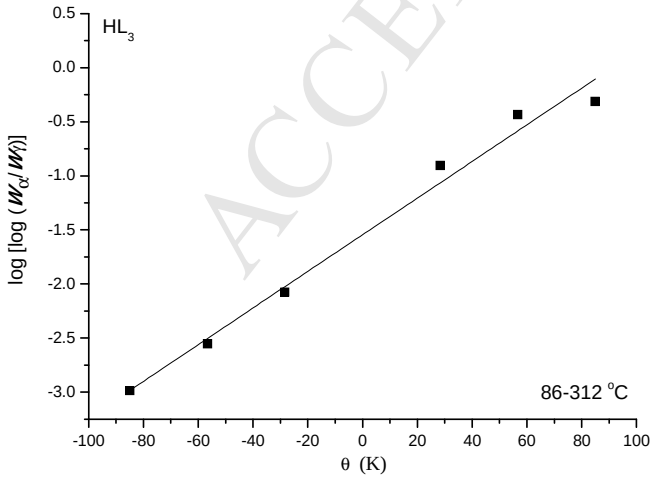

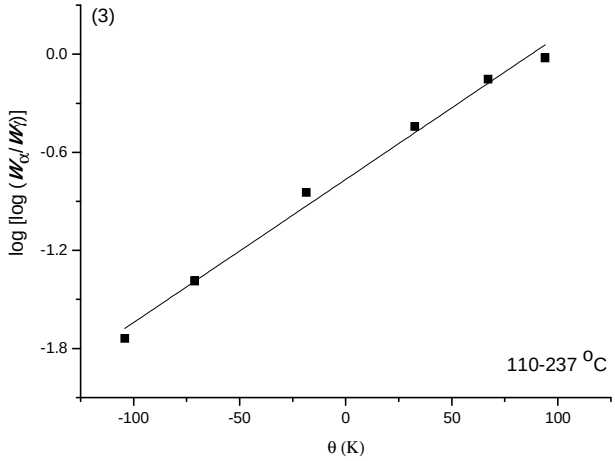

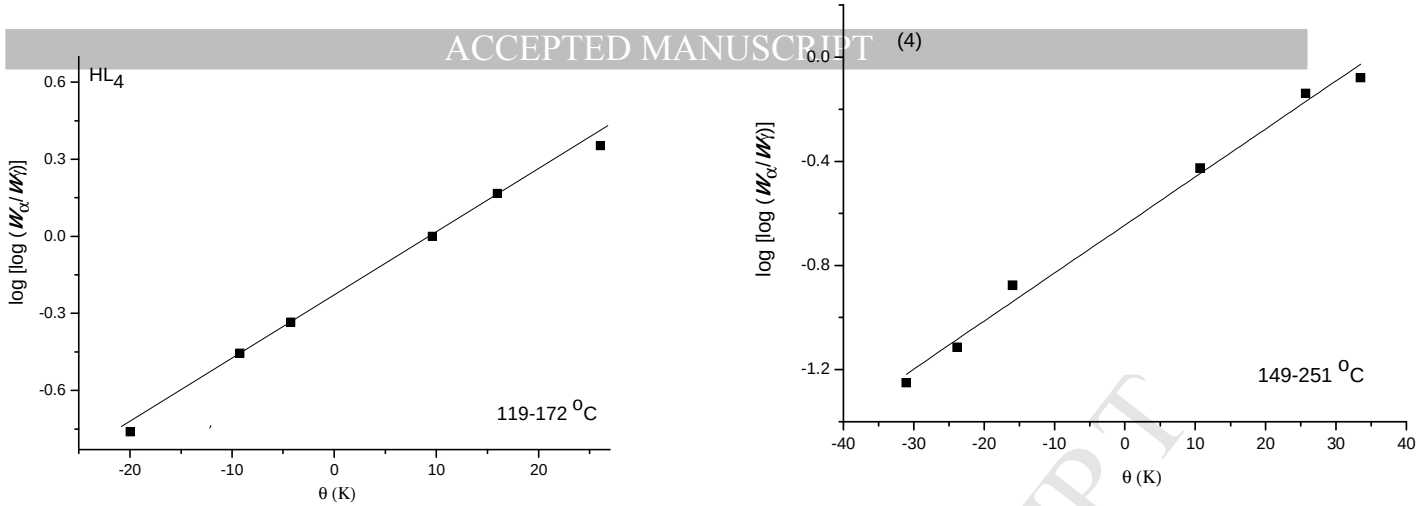

Fig. 7. Horowitz-Metzger (HM) of the ligands (**HL$_n$**) and their Cu(II) complexes (**1-4**).

HL_1

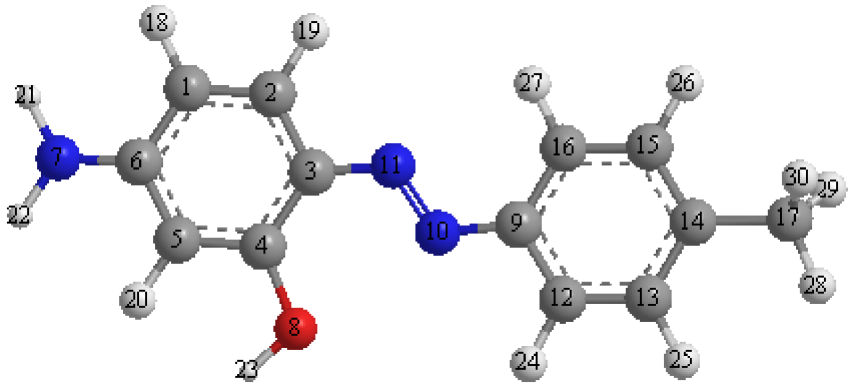

1

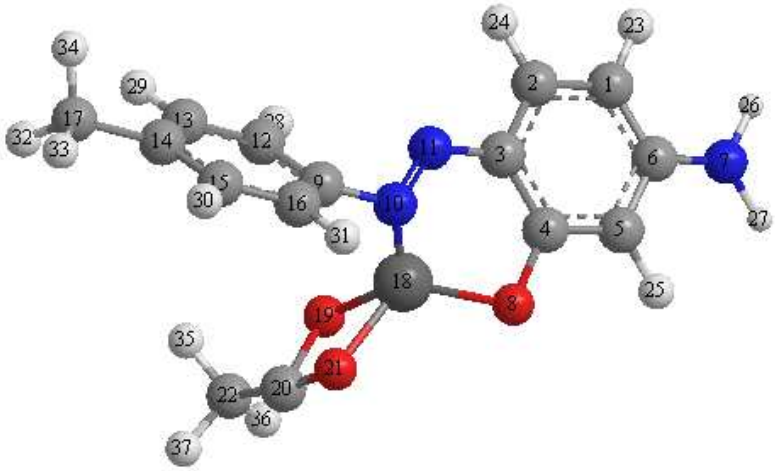

HL_2

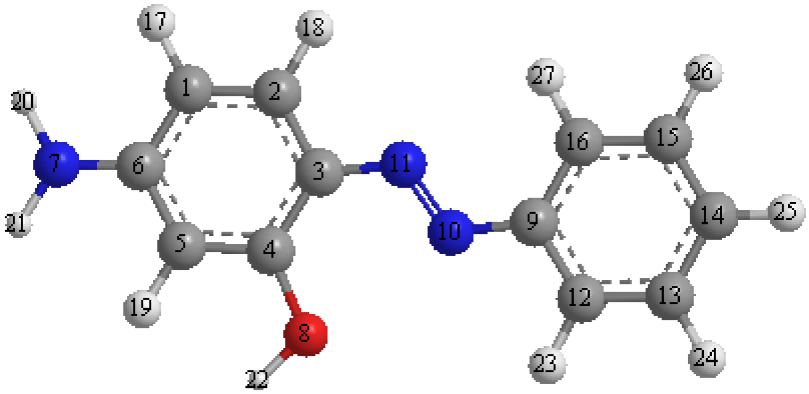

2

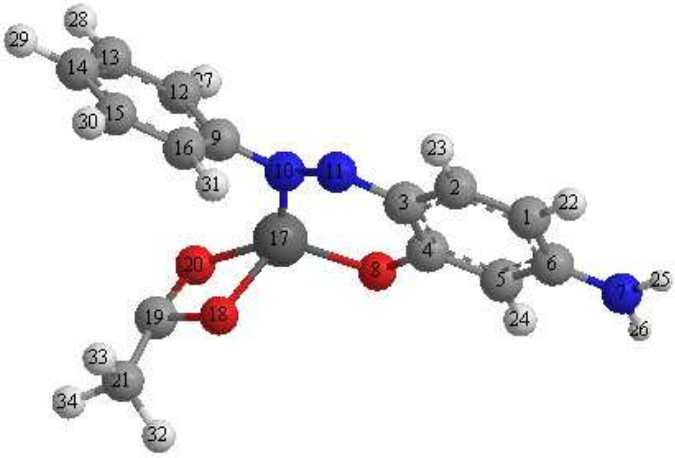

HL_3

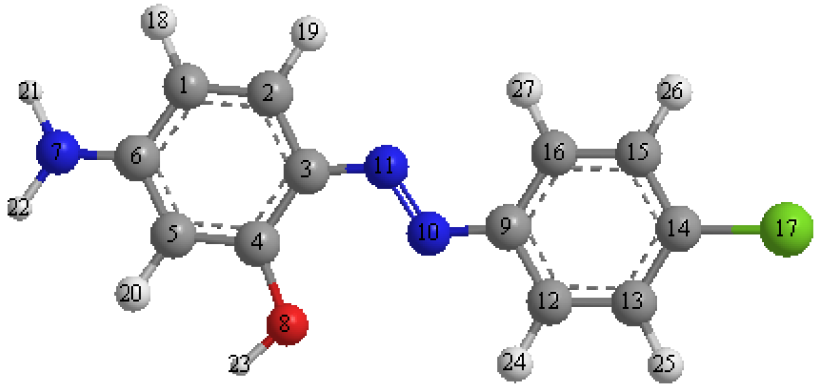

3

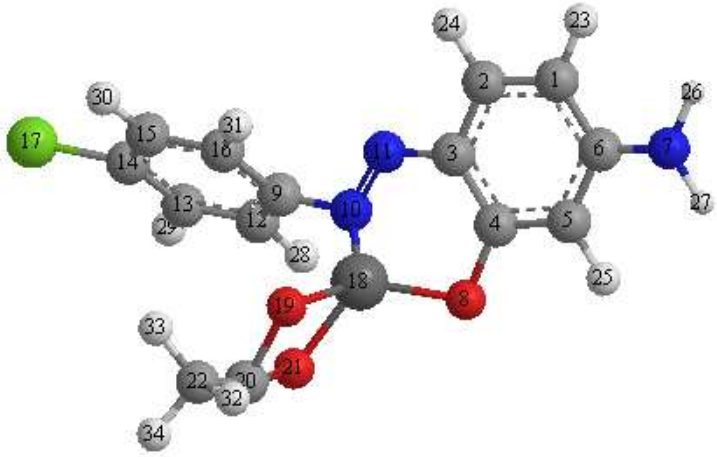

HL_4

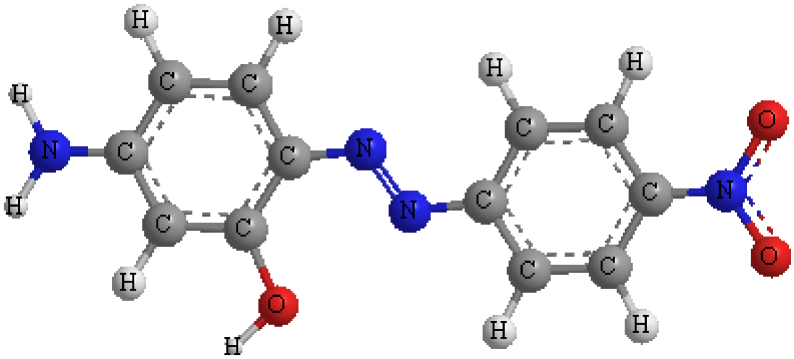

4

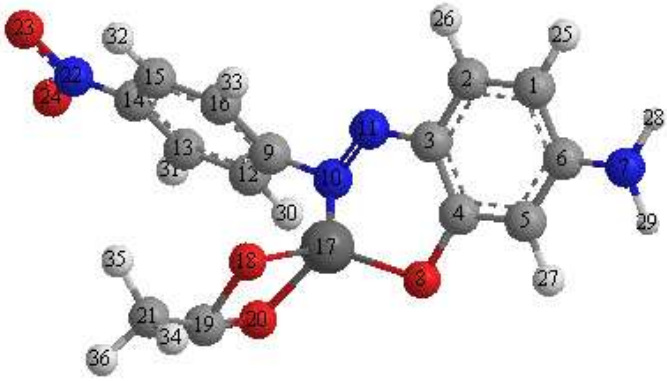

Fig. 8. The calculated molecular structures of the ligands (HL_n) and their complexes.

HL_1

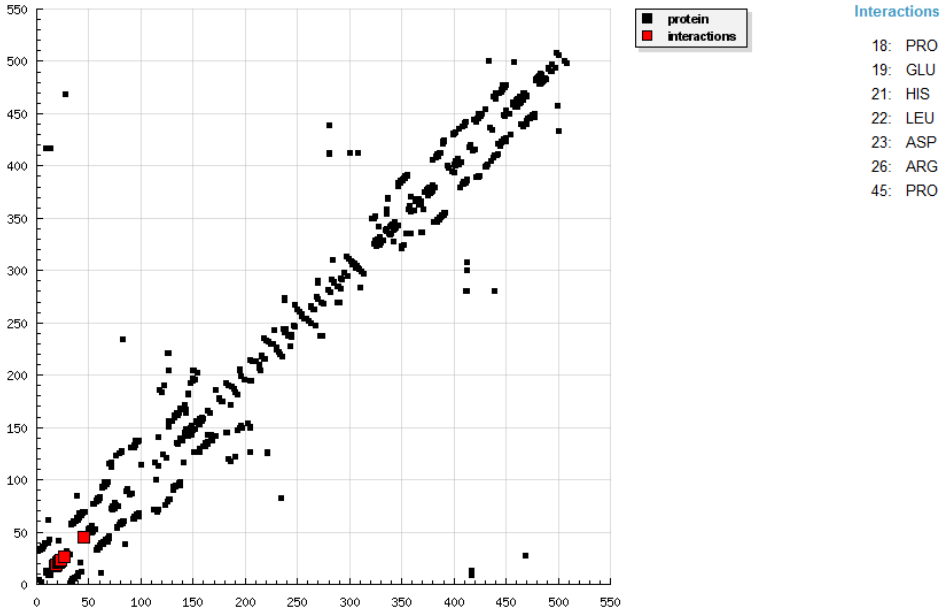
protein
interactions
Interactions
18: PRO
19: GLU
21: HIS
22: LEU
23: ASP
26: ARG
45: PRO

HL_2

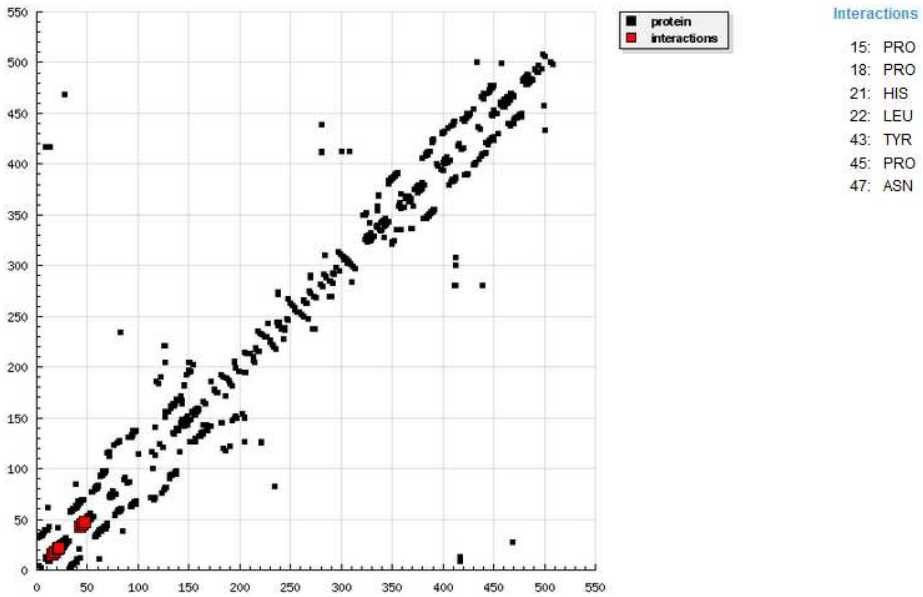
protein
interactions
Interactions
15: PRO
18: PRO
21: HIS
22: LEU
43: TYR
45: PRO
47: ASN

HL_3

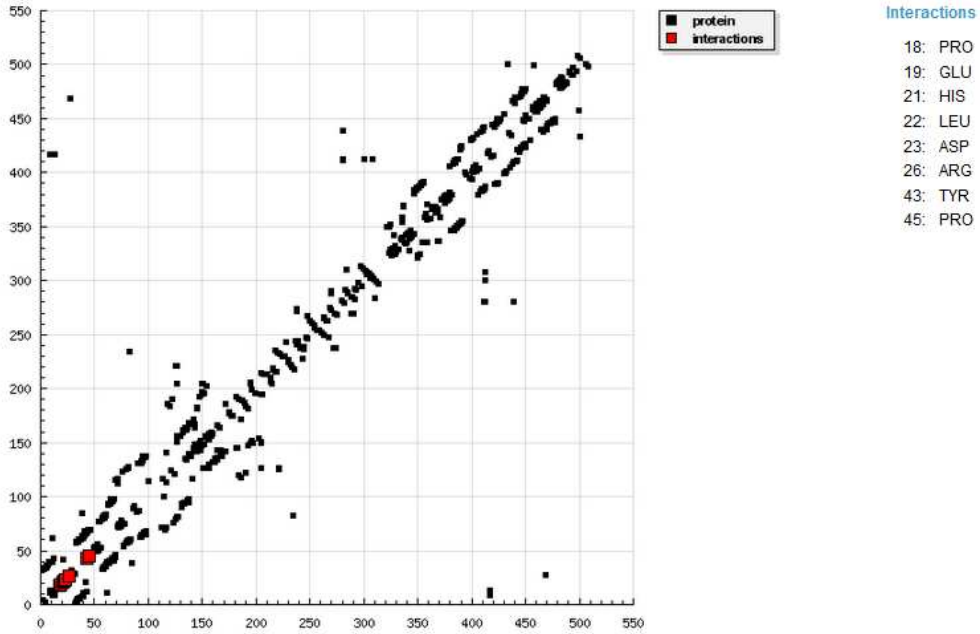

HL_4

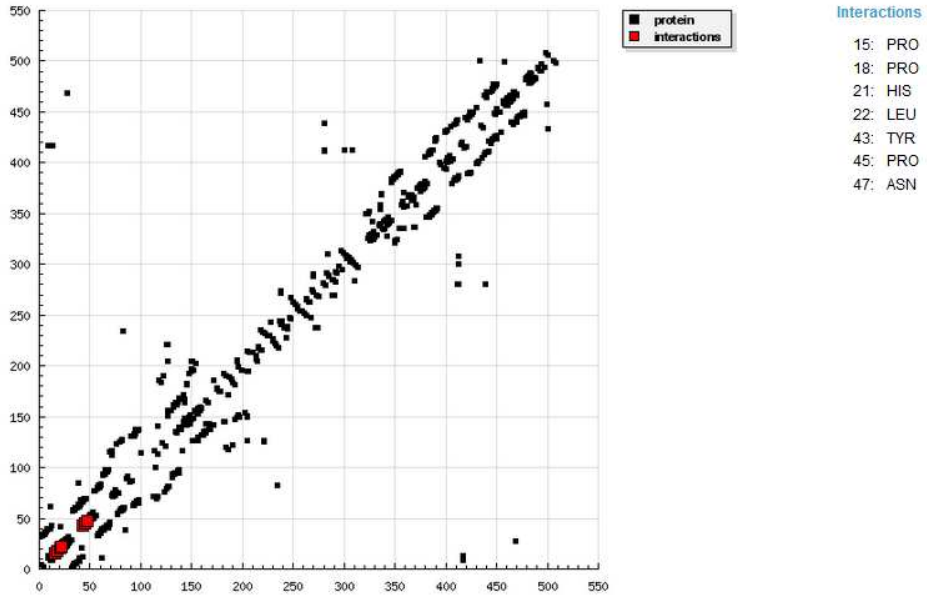

Fig. 9. HB plot of interaction between azo ligands and receptor 2a91

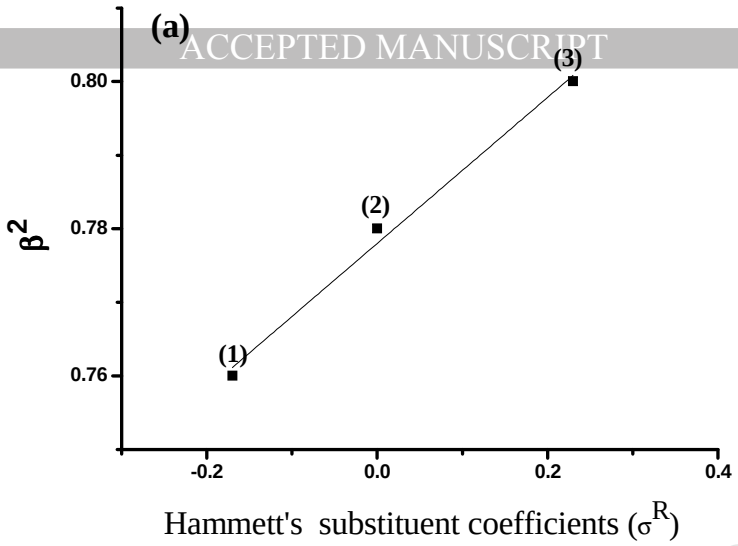

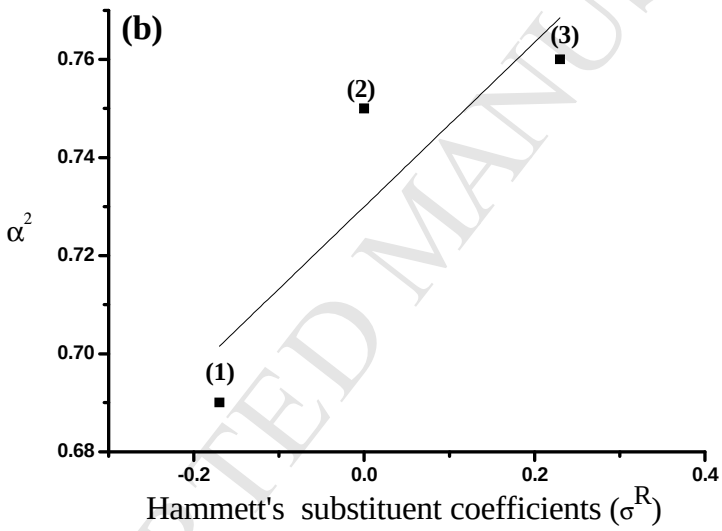

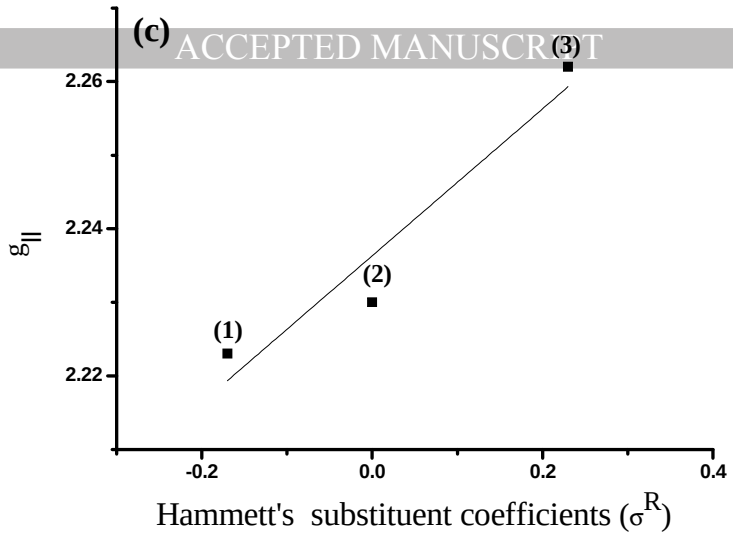

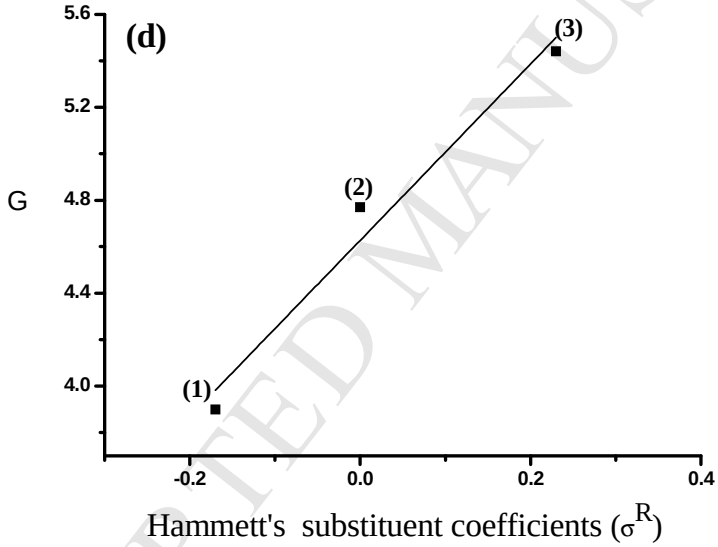

Fig. 10. The relation between Hammett's substituent coefficients (σ^R) *vs*. a) β^2, b) α^2, c) g_{II} and d) G of Cu(II) complexes **(1-3)**.

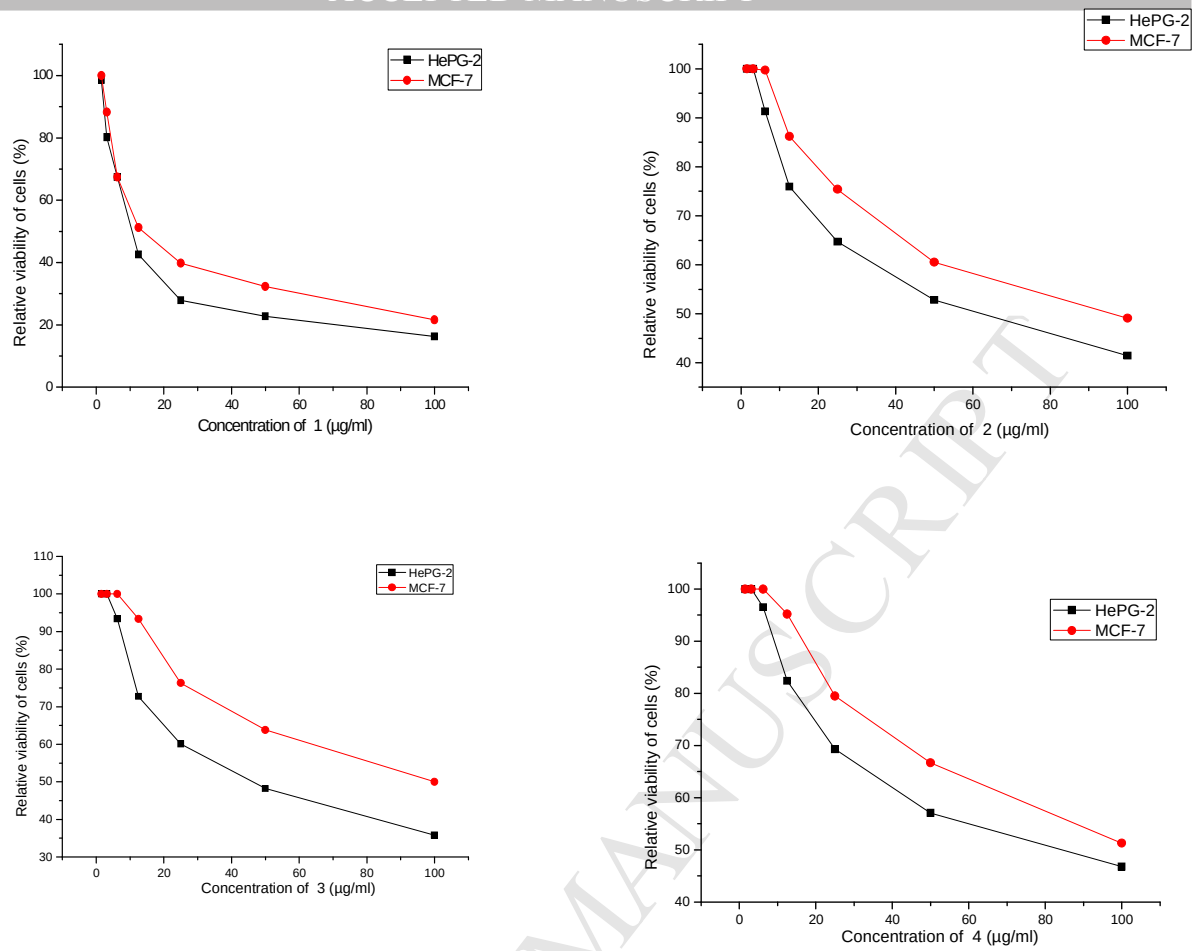

Fig. 11. Dose-response curves of the cytotoxicity of complexes (**1-4**). Each value represents the mean ± SD. Human hepatocellular carcinoma (HepG2), MCF-7.

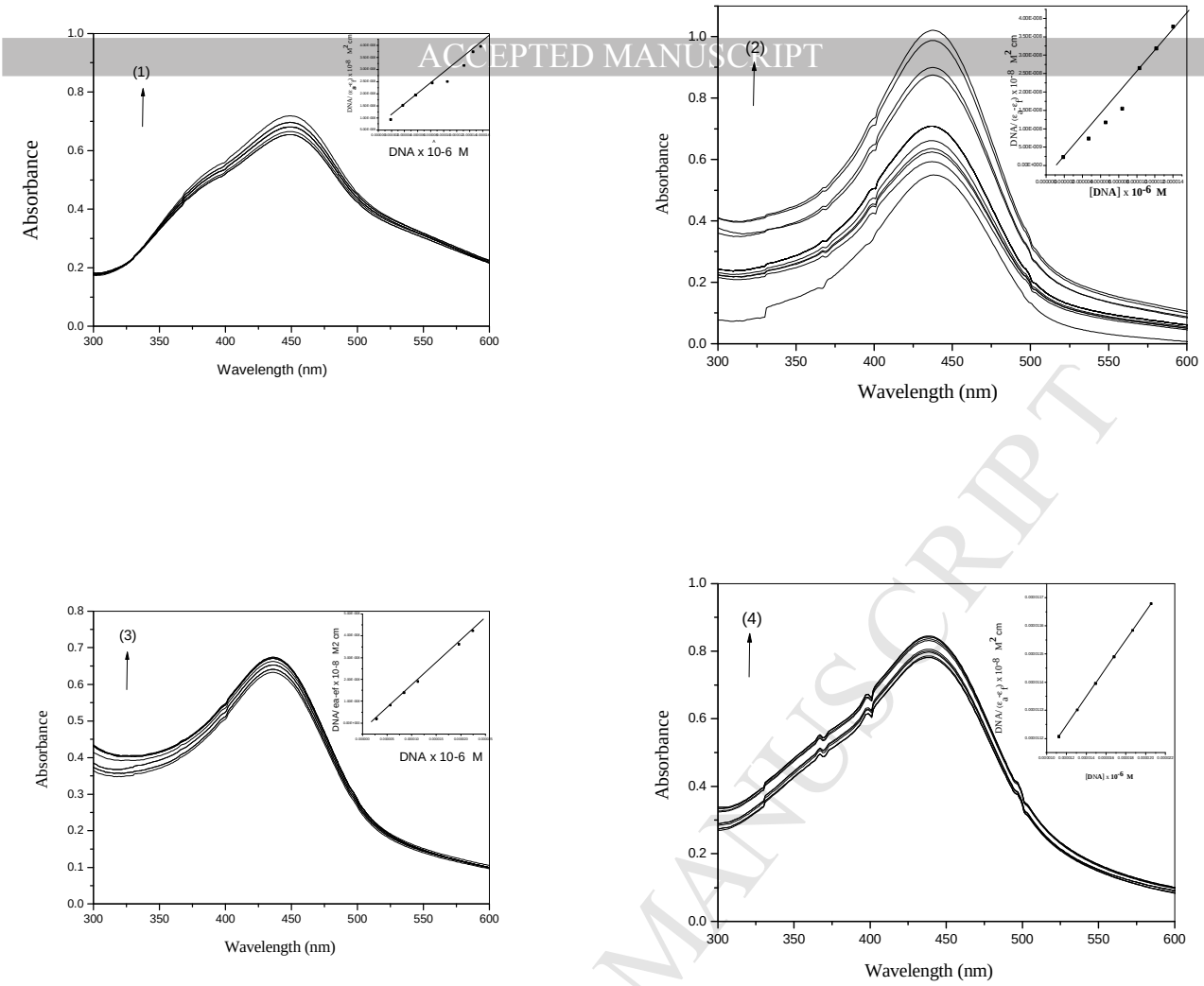

Fig. 12. Absorption spectra of complexes (**1-4**) in buffer pH 7.2 at 25 ^{o}C in the presence of increasing amount of CT-DNA. Arrows indicate the changes in absorbance upon increasing the CT-DNA concentration. Inset: plot of [DNA]/($\varepsilon_a - \varepsilon_f$) × 10^{-8} M^2 cm versus [DNA] × 10^{-6} M for titration of CT-DNA with complexes (**1-4**).

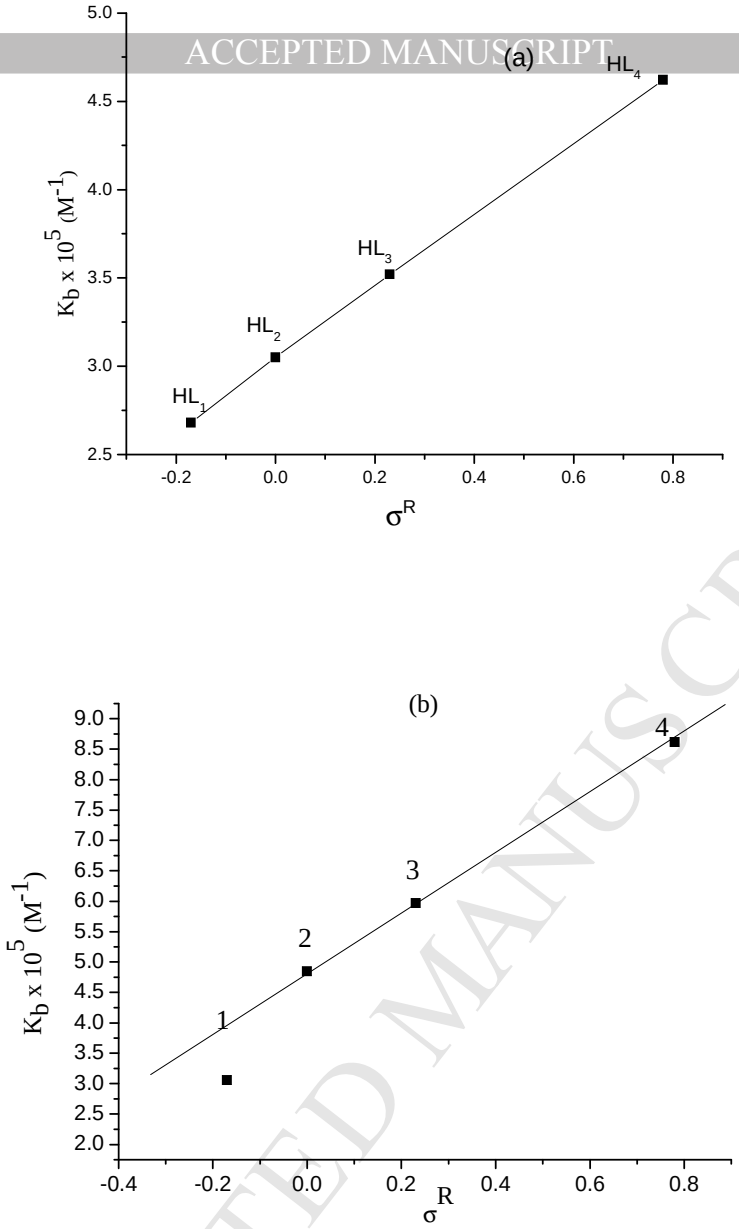

Fig. 13. The relation between Hammett's substitution coefficients (σ^R) *vs.* intrinsic binding constants (K_b) of the a) ligands (**HL_n**) and b) Cu(II) complexes (**1-4**).

- Copper(II) complexes of azo amino phenol are prepared and characterized
- Quantum chemical parameters of copper(II) complexes of azo amino phenol are calculated
- The activation energies of the degradation of the Cu(II) complexes are calculated